Interannual variations in δ(APO) and δ(Ar/N_2) at the surface and gravitational separation in the stratosphere

Shigeyuki Ishidoya[1], Satoshi Sugawara[2], Yasunori Tohjima[3], Daisuke Goto[4], Shinji Morimoto[5], Kazuhiro Tsuboi[6], Shohei Murayama[1], Kentaro Ishijima[6], Nobuyuki Aoki[1], Yosuke Niwa[3], Sakae Toyoda[7], Hideyuki Honda[5], Shuji Aoki[5], Takakiyo Nakazawa[5], Yoichi Inai[8], Fumio Hasebe[9]

1:National Institute of Advanced Industrial Science and Technology (AIST),
2:Miyagi University of Education, 3:National Institute for Environmental Studies,
4:National Institute of Polar Research, 5:Tohoku University, 6:Meteorological Research Institute,
7:Tokyo Institute of Technology, 8:Japan Meteorological Agency, 9:Hokkaido University

Outline

Brief introduction of our recent project

Variations in Ar/N_2 and APO at some surface stations since 2012

Gravitational separation in the stratosphere over Japan since 1988

Combined analysis of the surface and the stratospheric Ar/N_2 trends

Outline

Brief introduction of our recent project

Variations in Ar/N_2 and APO at some surface stations since 2012

Gravitational separation in the stratosphere over Japan since 1988

Combined analysis of the surface and the stratospheric Ar/N_2 trends

In our project, Grant-in-Aid for Scientific Research (S), JSPS, we propose methods to evaluate changes in ocean heat content, atmospheric circulation, and carbon/oxygen cycles based on wide-area observations of atmospheric constituents; O_2/N_2, Ar/N_2 and their $\delta^{18}O$, $\delta^{15}N$ and $\delta^{40}Ar$, concentrations of CO_2 and COS and its $\delta^{34}S$.

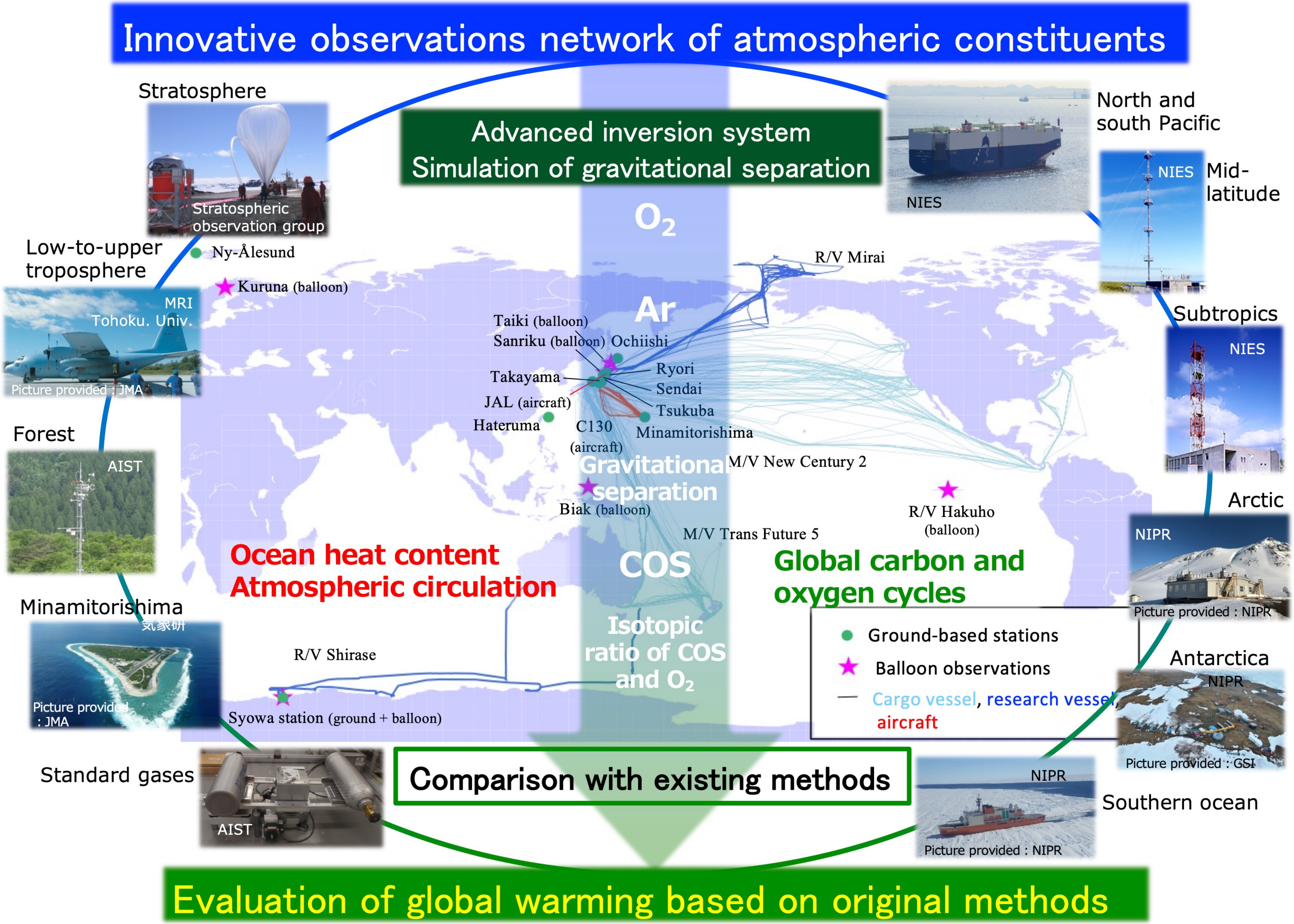

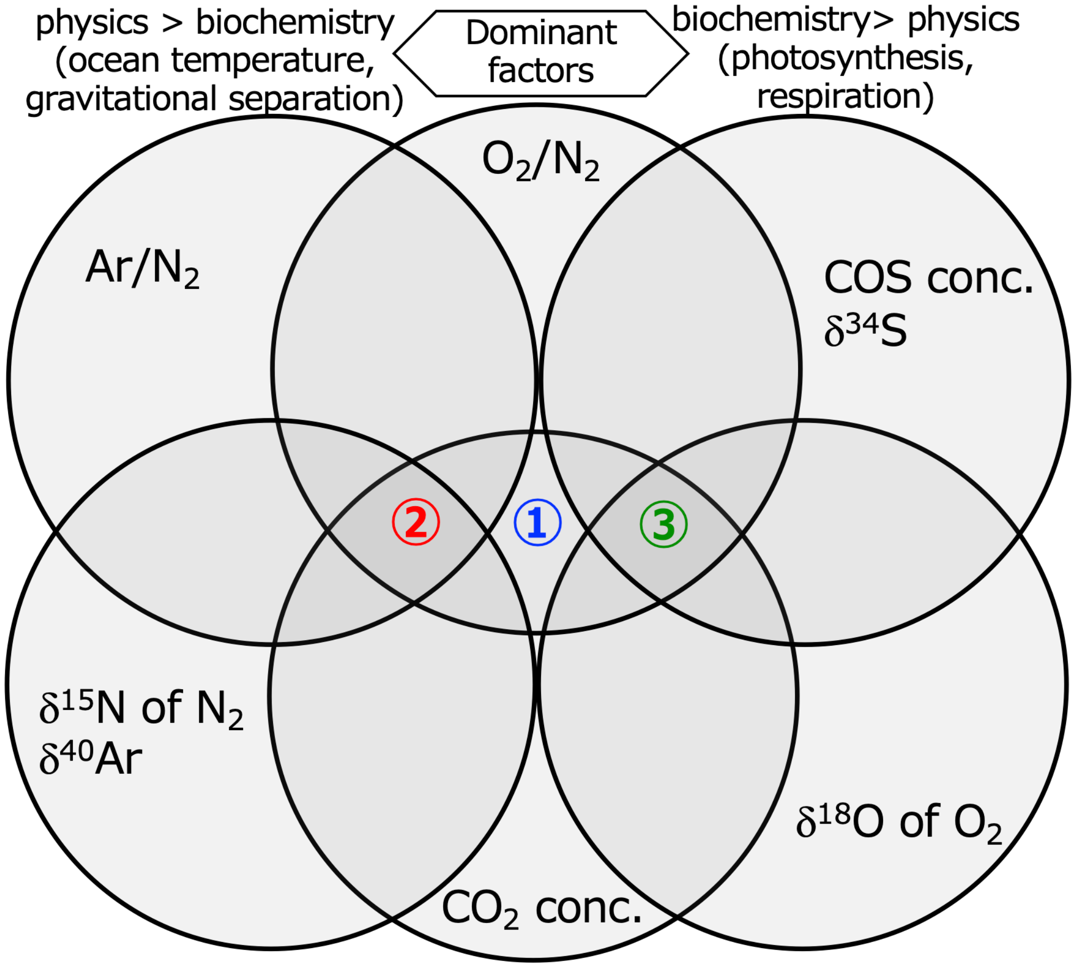

①net CO_2 uptake = O_2+CO_2
②ocean heat content & net marine biological activities
= Ar+O_2+gravitational separation ($\delta^{15}N$ etc.)+CO_2
③Photosynthesis・respiration = COS+$\delta^{18}O$+O_2+CO_2

Image of the combined analyses using multi species

O_2/N_2 and Ar/N_2 have information about global CO_2 cycle and air-sea heat flux, respectively, but their variations are quite small. An effect of stratospheric gravitational separation should also be considered to discuss a secular trend of Ar/N_2.

COS and $\delta^{18}O$ of O_2 have information about photosynthesis and respiration, however, development of stable standard is needed for COS, and $\delta^{18}O$ change in the present atmosphere has never been detected.

In this regard, all Japanese institutes capable of measuring the above-mentioned components, and National Metrology Institute participate in this research project. Moreover, modelers capable of carrying out advanced inversion analyses and simulation of gravitational separation also join us. Therefore, we are going to promote this project.

Outline

Brief introduction of our recent project

Variations in Ar/N_2 and APO at some surface stations since 2012

Gravitational separation in the stratosphere over Japan since 1988

Combined analysis of the surface and the stratospheric Ar/N_2 trends

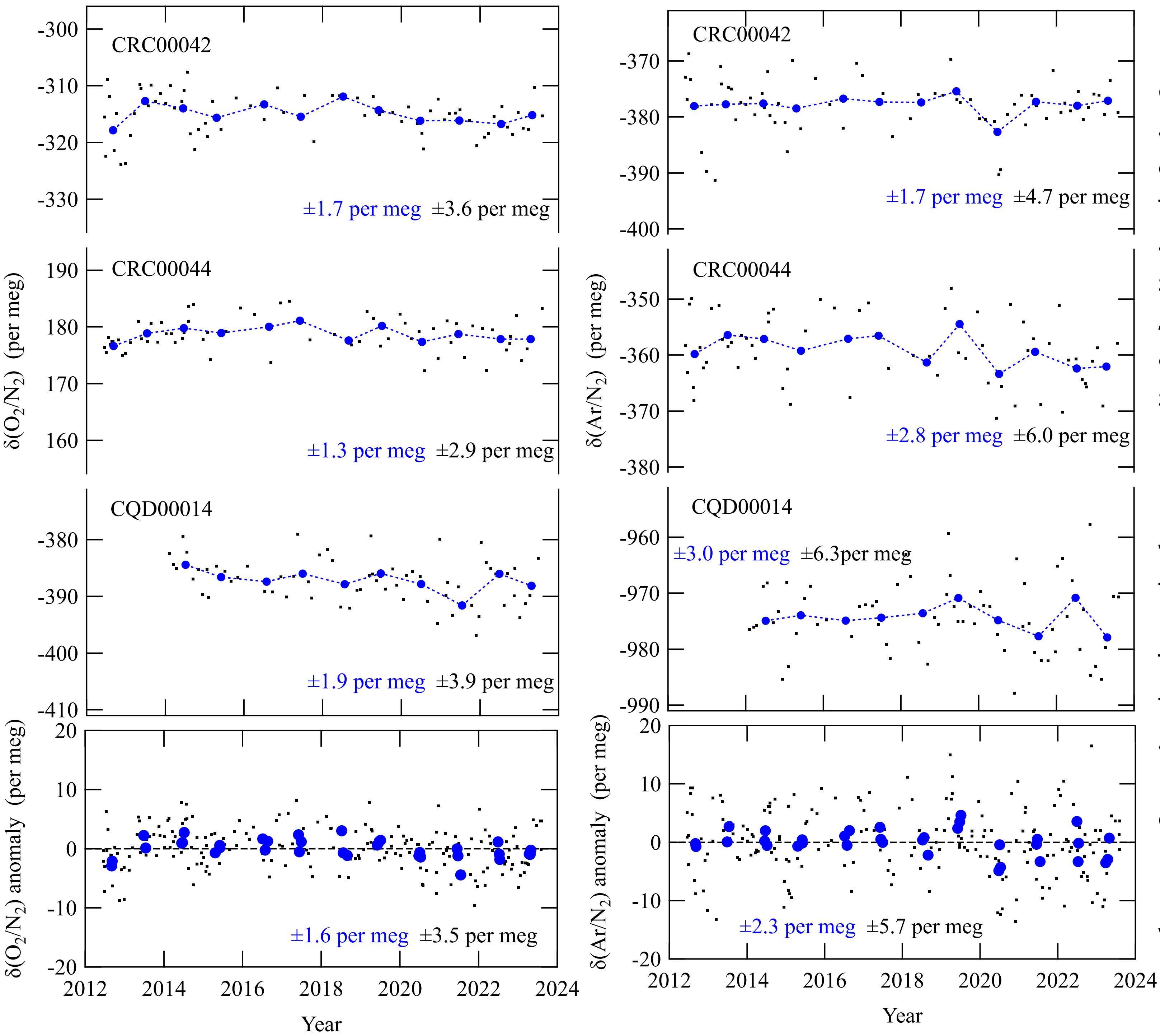

Each analysis value (black dots) and corresponding annual average (blue circles) of $\delta(O_2/N_2)$ and $\delta(Ar/N_2)$ of three secondary standards against the primary standard air.

Anomalies of $\delta(O_2/N_2)$ and $\delta(Ar/N_2)$ of the three secondary standards shown in bottom panels.

No systematic temporal variations are found over the 11 years.

The standard deviations of the annual average $\delta(O_2/N_2)$ and $\delta(Ar/N_2)$ anomalies ($\pm$1.6 and $\pm$2.3 per meg) corresponds to $\pm$0.20 and $\pm$0.29 per meg yr^{-1}, respectively, for the 11-year-long secular trends.

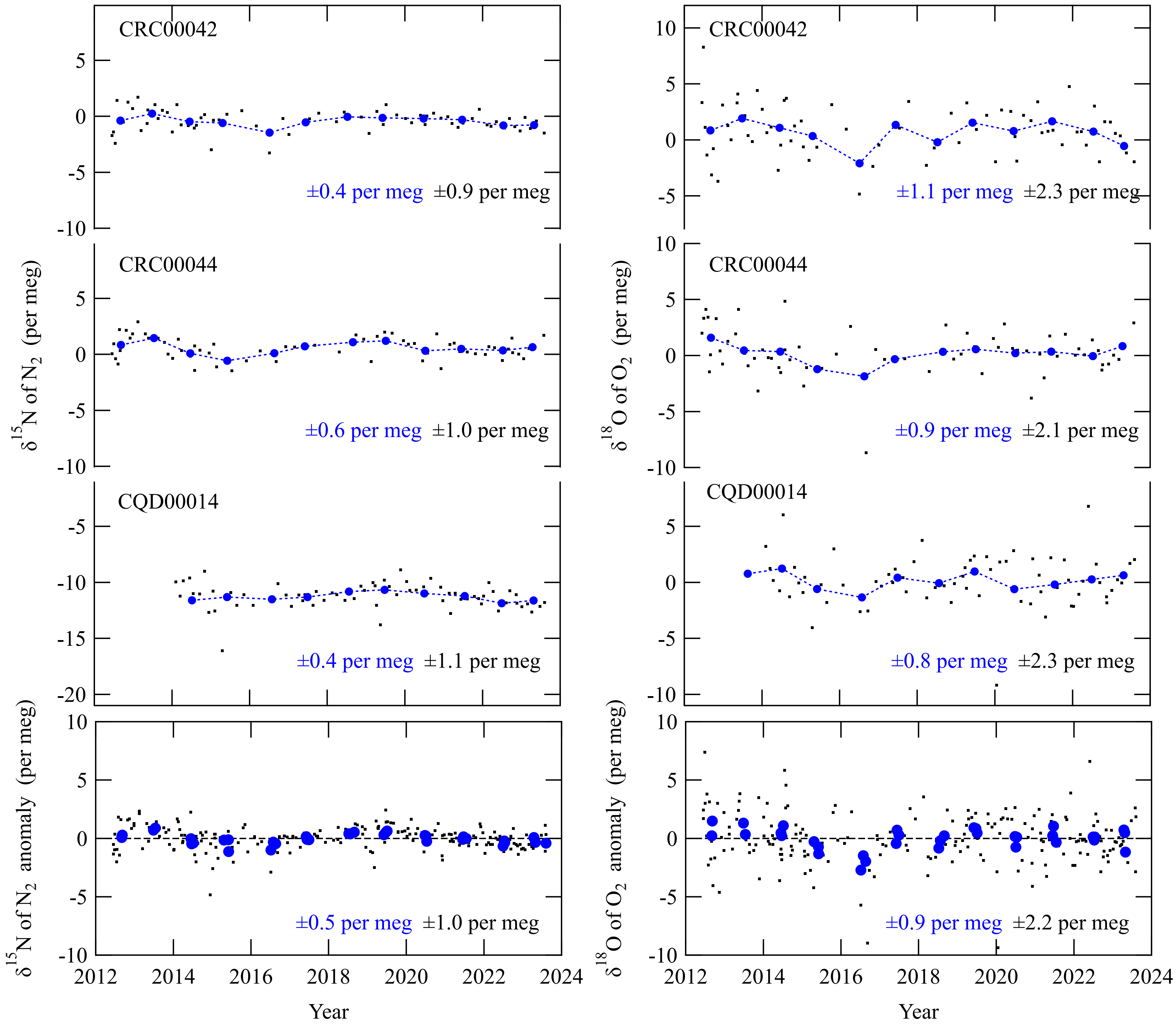

The same as in the previous figures but for $\delta^{15}N$ of N_2 and $\delta^{18}O$ of O_2.

No systematic temporal variations are found over the 11 years.

The standard deviations of the annual average $\delta^{15}N$ and $\delta^{18}O$ anomalies (±0.5 and ±0.9 per meg) corresponds to ±0.06 and ±0.11 per meg yr^{-1}, respectively, for the 11-year-long secular trends.

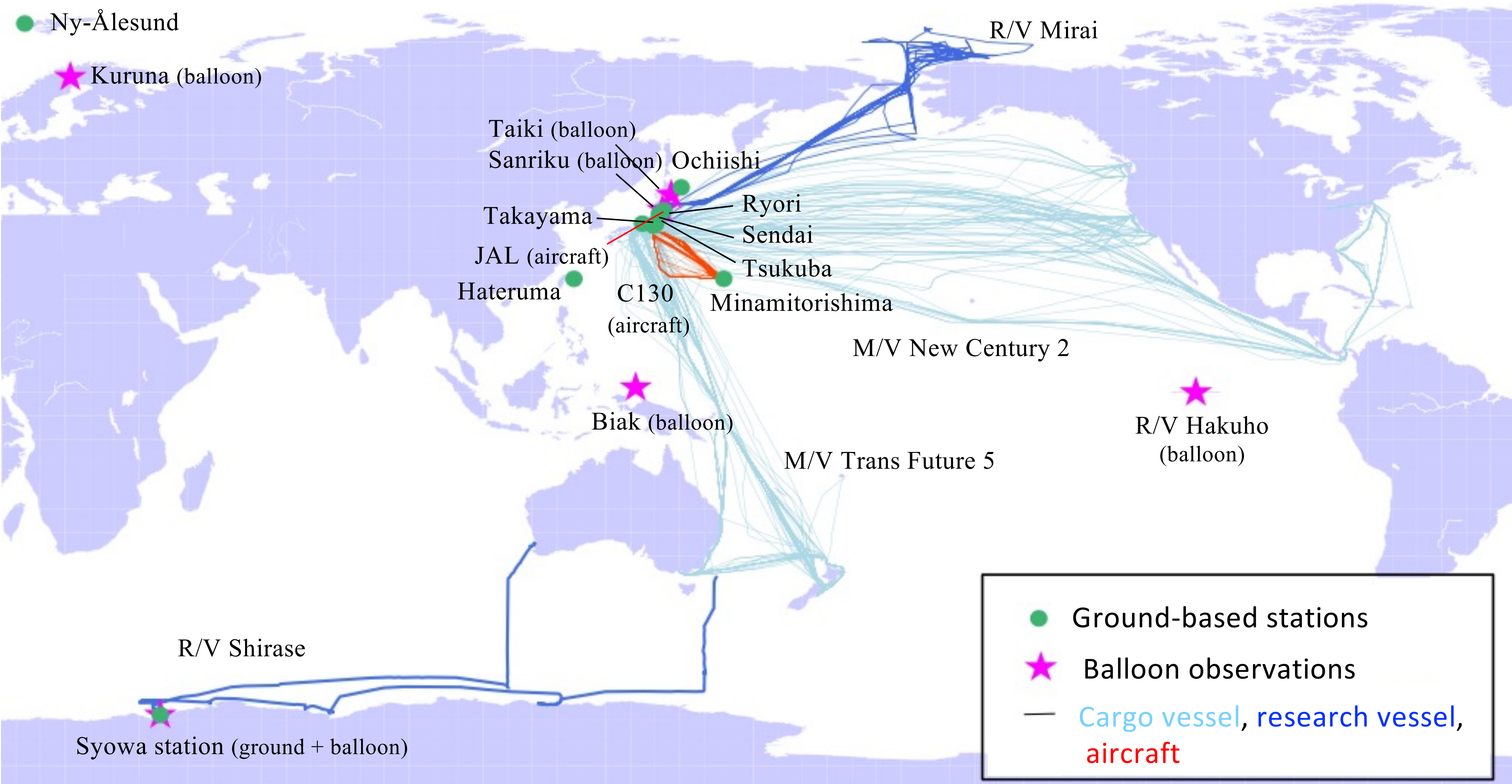

Ny-Ålesund
Kuruna (balloon)
R/V Mirai
Taiki (balloon)
Sanriku (balloon)
Ochiishi
Ryori
Takayama
Sendai
JAL (aircraft)
Tsukuba
Hateruma
C130 (aircraft)
Minamitorishima
M/V New Century 2
Biak (balloon)
R/V Hakuho (balloon)
M/V Trans Future 5
R/V Shirase
Syowa station (ground + balloon)
Ground-based stations
Balloon observations
Cargo vessel, research vessel, aircraft

Our surface stations where we have conducted simultaneous observations of δ(APO) and δ(Ar/N_2)

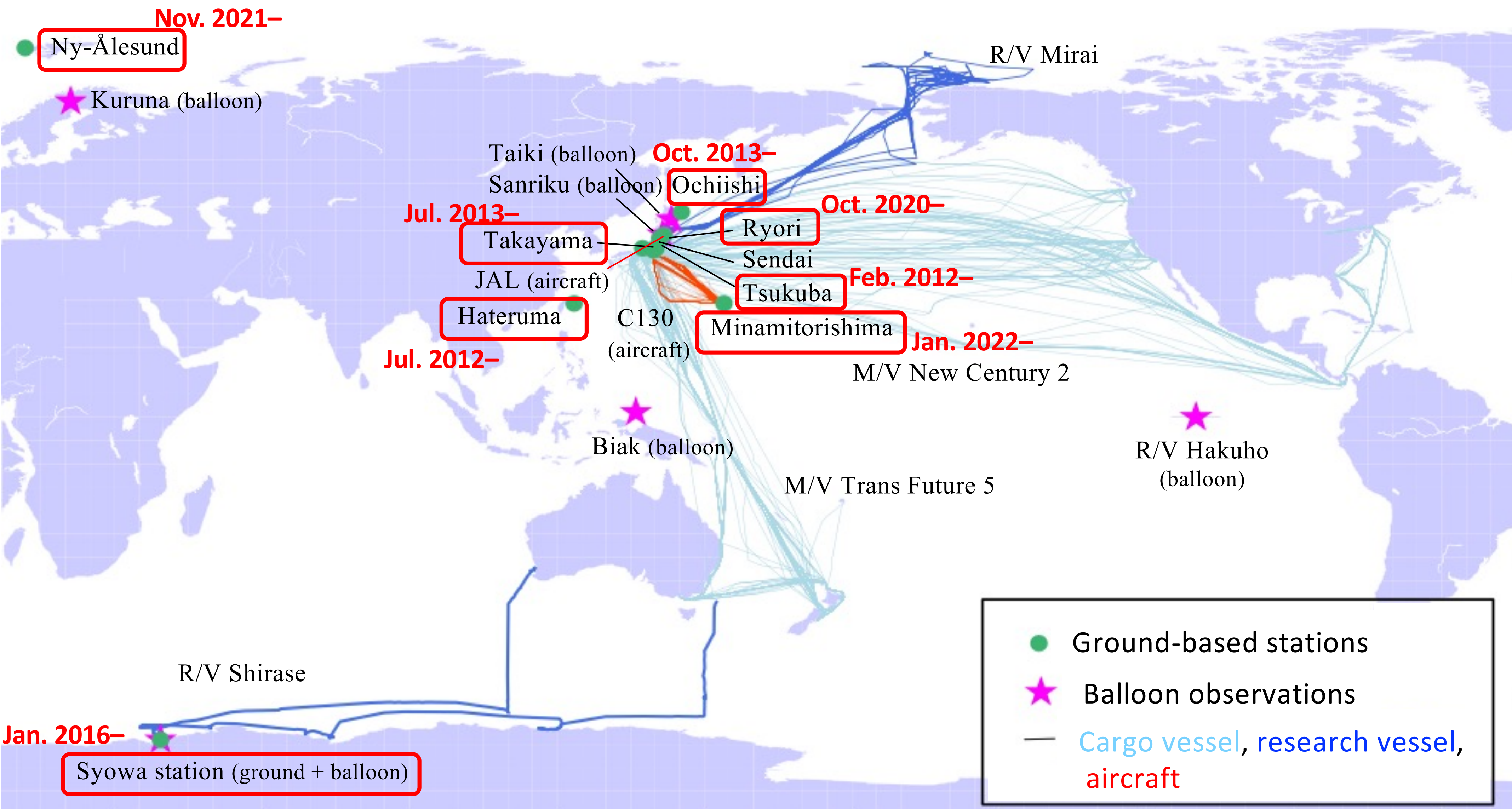

Our surface stations where we have conducted simultaneous observations of δ(APO) and δ(Ar/N_2)

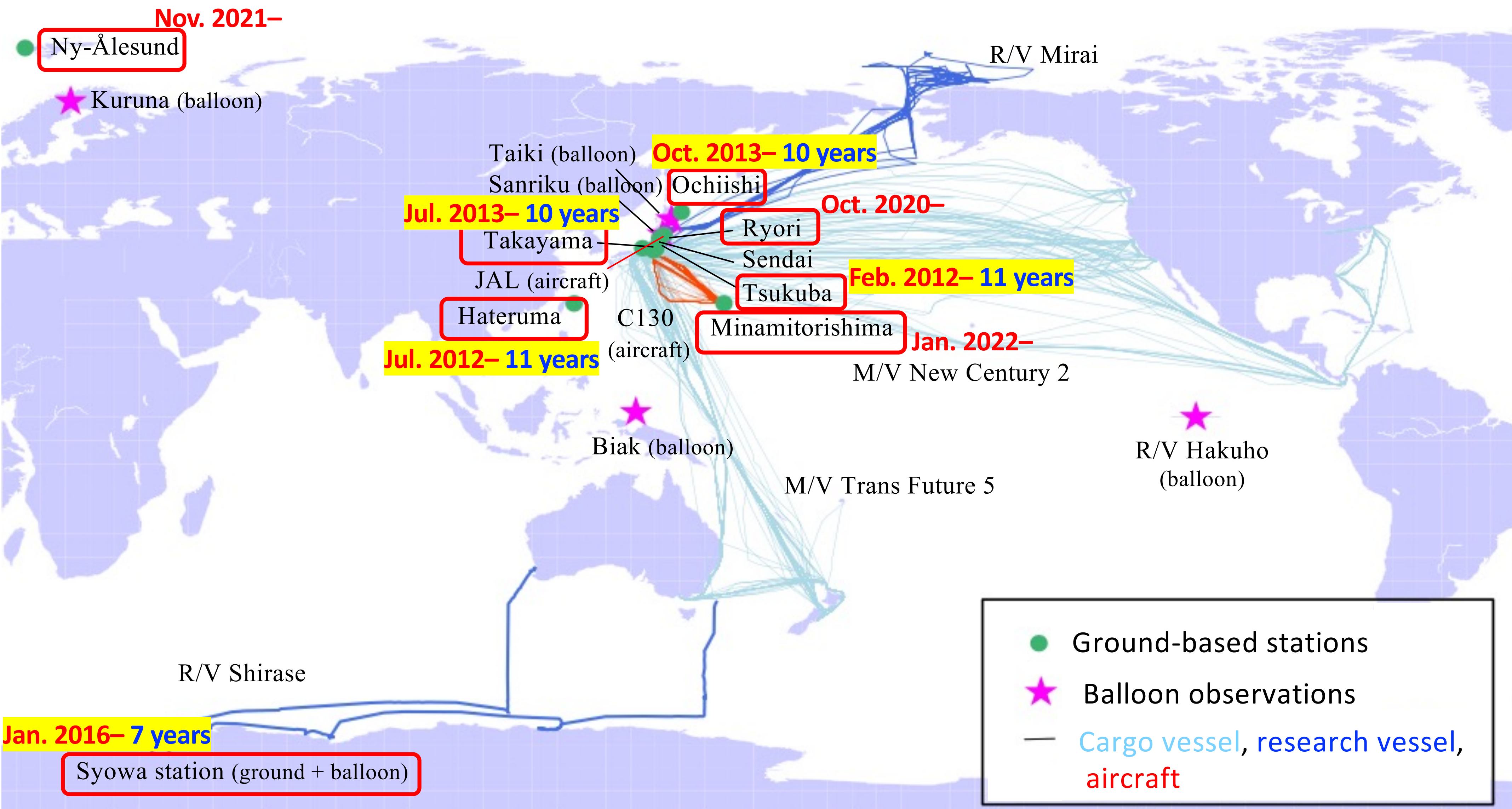

Our surface stations where we have conducted simultaneous observations of δ(APO) and δ(Ar/N_2)

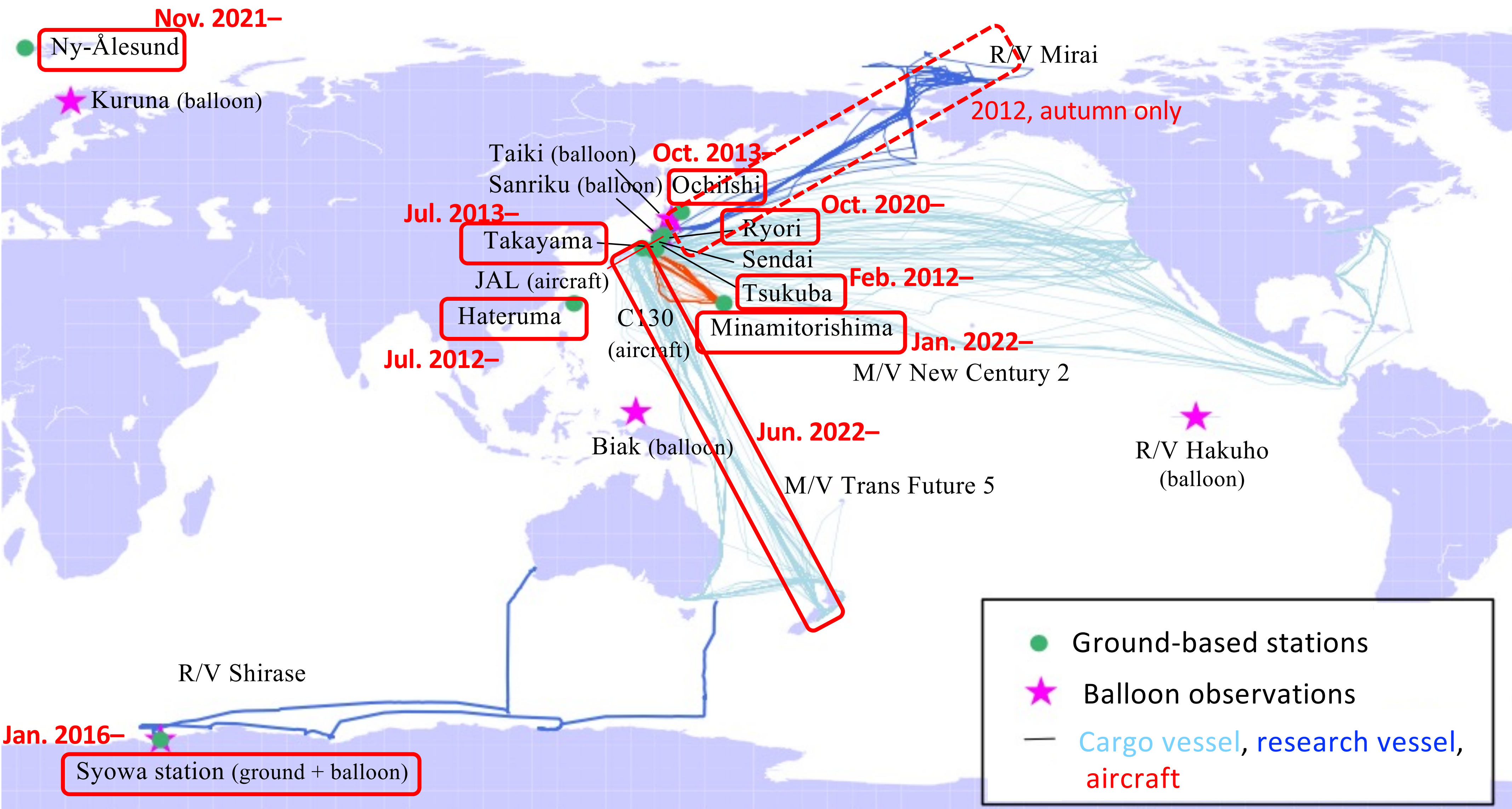

We have also expanded the observation area using a merchant or a research vessels.

Variations in δ(APO) and δ(Ar/N_2) observed at Tsukuba (TKB), Hateruma (HAT), Ochiishi (COI), Minamitorishima (MNM), and Ryori (RYO), Japan

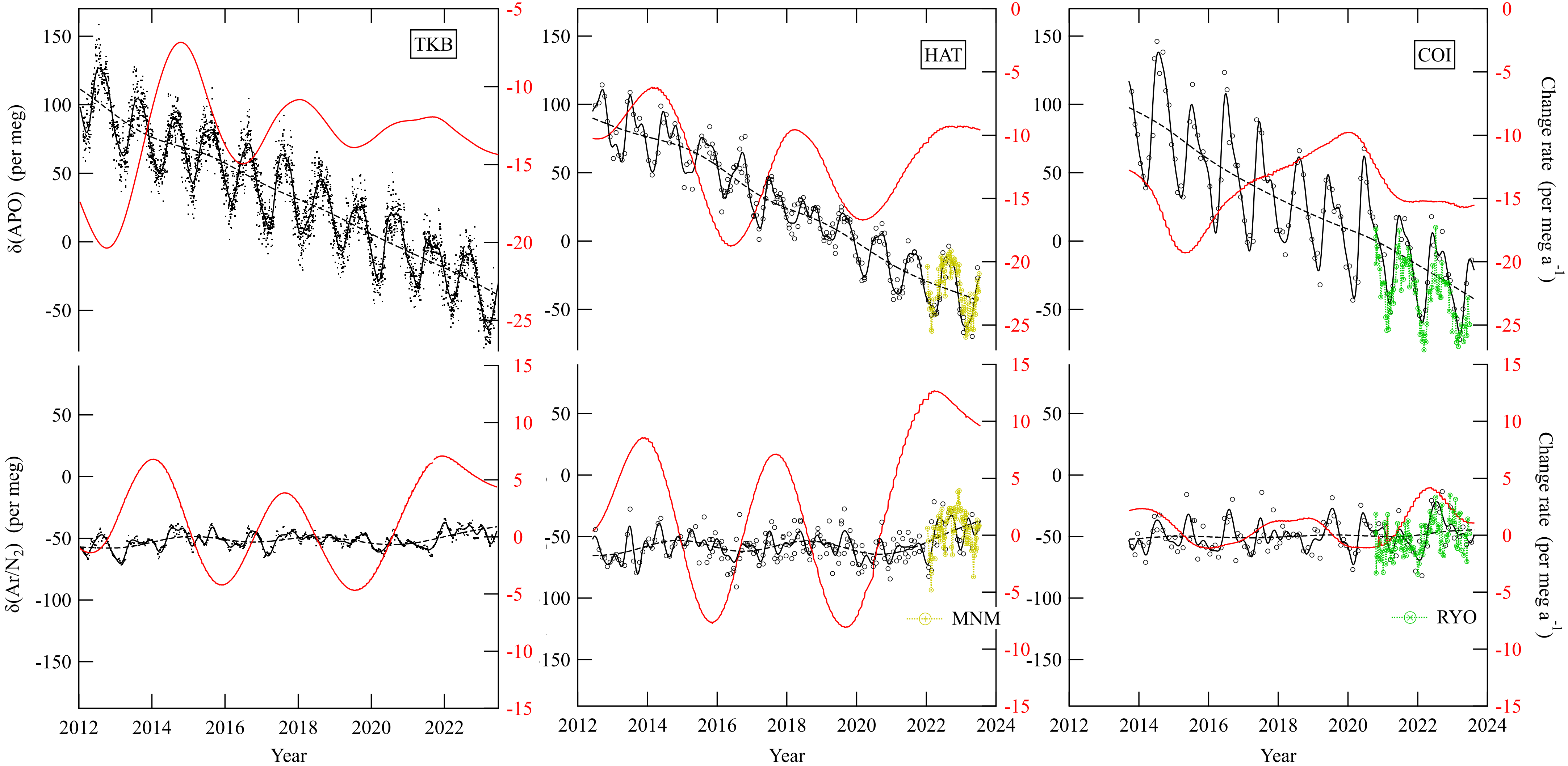

Temporal variations of δ(APO) and δ(Ar/N_2) at Tsukuba, Hateruma, and Ochiishi, Japan. Best-fit curves to the data (solid lines) and interannual variations (dashed lines) are also shown. Rates of change of δ(APO) and δ(Ar/N_2) are also shown by red lines (cutoff period is 36 months to obtain the interannual variation). The data observed at Minamitorishima and Ryori located at close latitude to Hateruma and Ochiishi, respectively, are also shown. Since Tsukuba is urban site, the APO data affected by local fossil fuel consumption were excluded from the analysis.

Variations in δ(APO) and δ(Ar/N_2) observed at TKB, HAT, COI, MNM, RYO, Takayama (TKY), Japan and Syowa (SYO), Antarctica

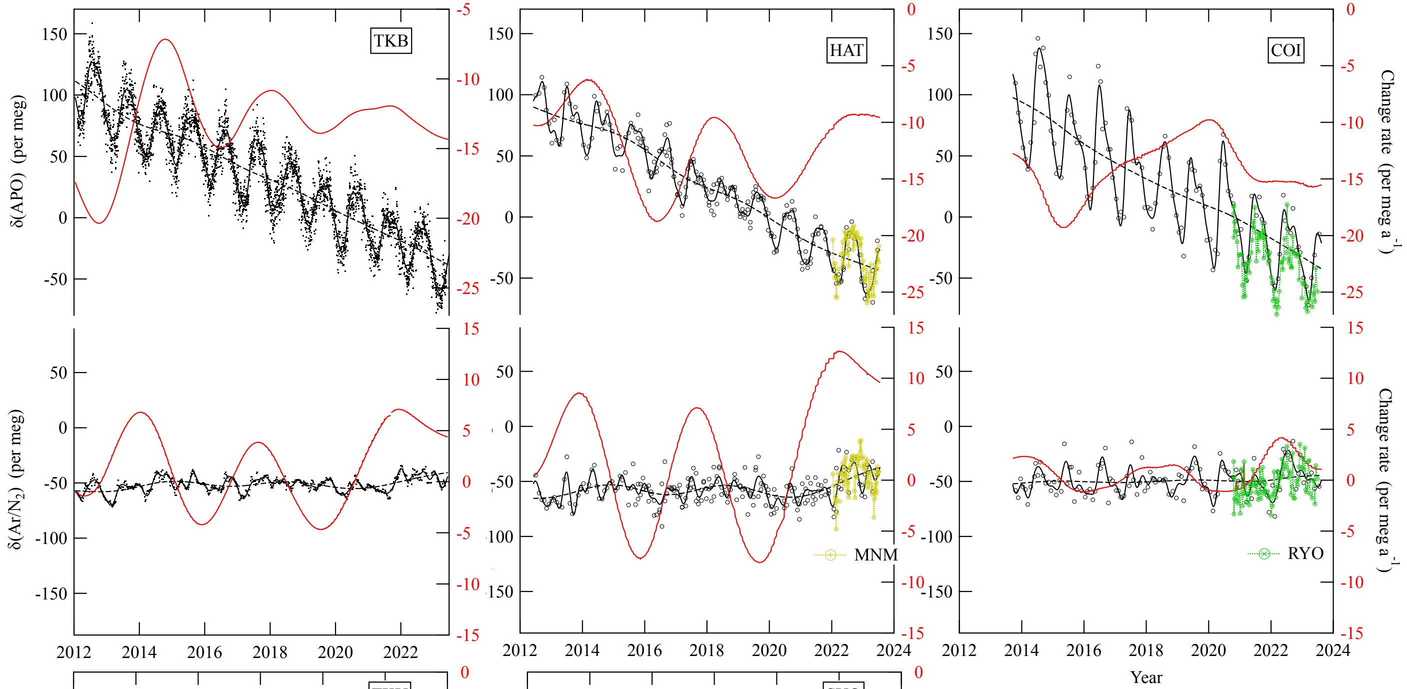

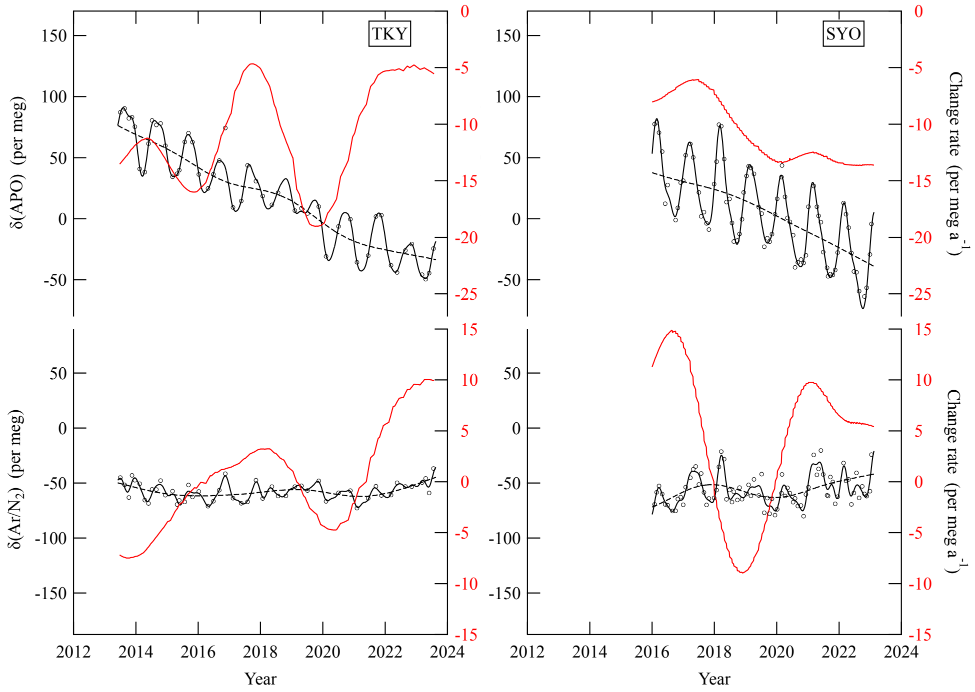

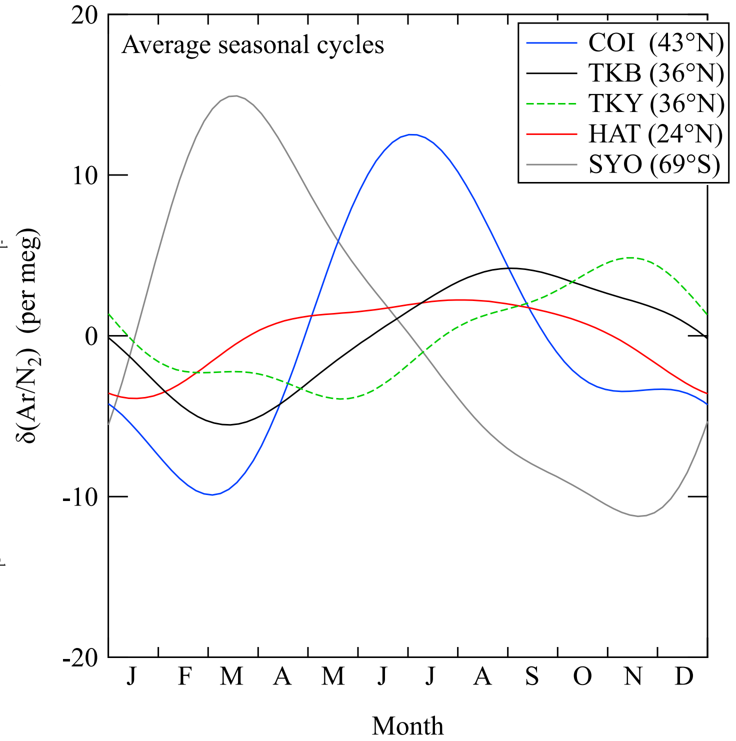

Temporal variations at Takayama and Syowa are also shown in this slide. The average seasonal δ(Ar/N_2) cycles (upper right figure) show summer to autumn maxima in both hemispheres, and the seasonal amplitudes are larger at higher latitude.

We have recognized our δ(Ar/N_2) data are somewhat noisier than those reported by Scripps O_2 program. So, I am now trying to improve our measurements using a new mass spectrometer.

Annual change rate of δ(APO) due to the solubility change (δ(APO)$_{therm}$) from that due to the net marine biological activities (δ(APO)$_{netbio}$) by a combined analysis of δ(APO) and δ(Ar/N_2).

Bottom figure shows change rates of
δ(APO)
δ(APO)$_{therm}$ =δ(Ar/N_2) x 0.9
δ(APO)$_{netbio}$ + fossil fuel + air-sea CO_2 exchange = δ(APO) - δ(APO)$_{therm}$.

Right figure shows the rates and some climate indexes (discussed below).

* It is known that the seasonal and interannual variations in δ(APO) are driven mainly by the air-sea O_2 and N_2 fluxes, although the air-sea CO_2 and fossil fuel fluxes cause a secular δ(APO) trend.

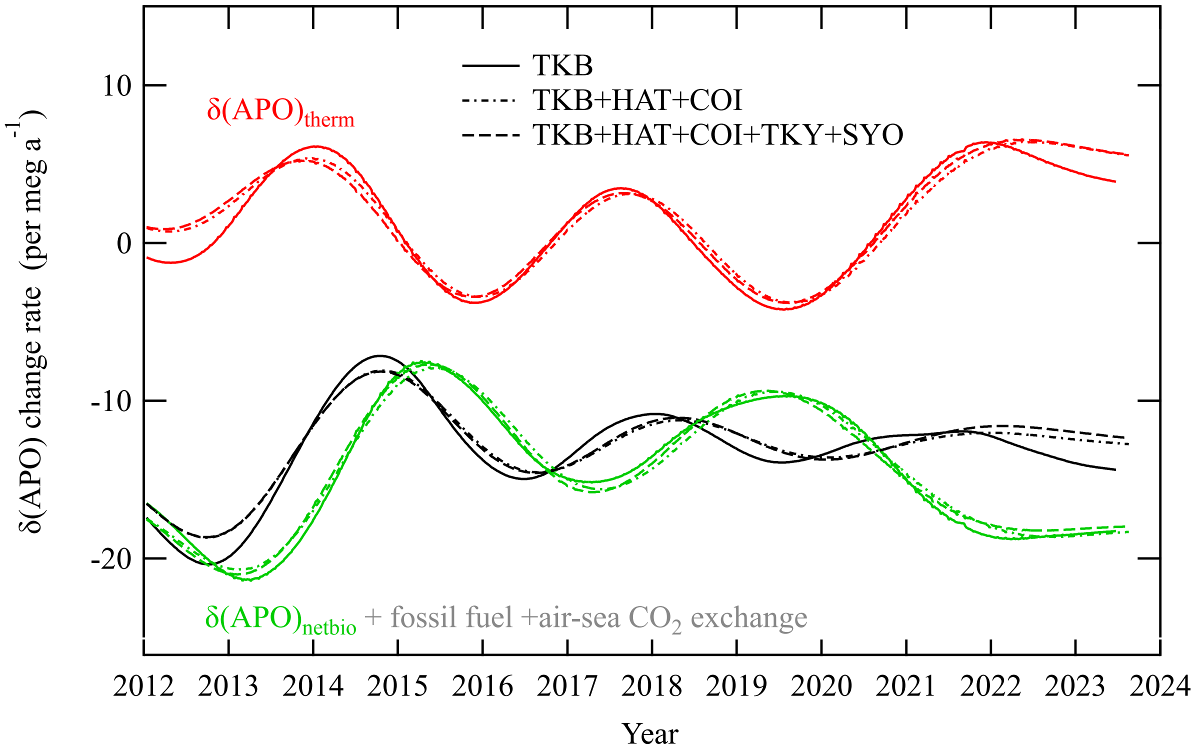

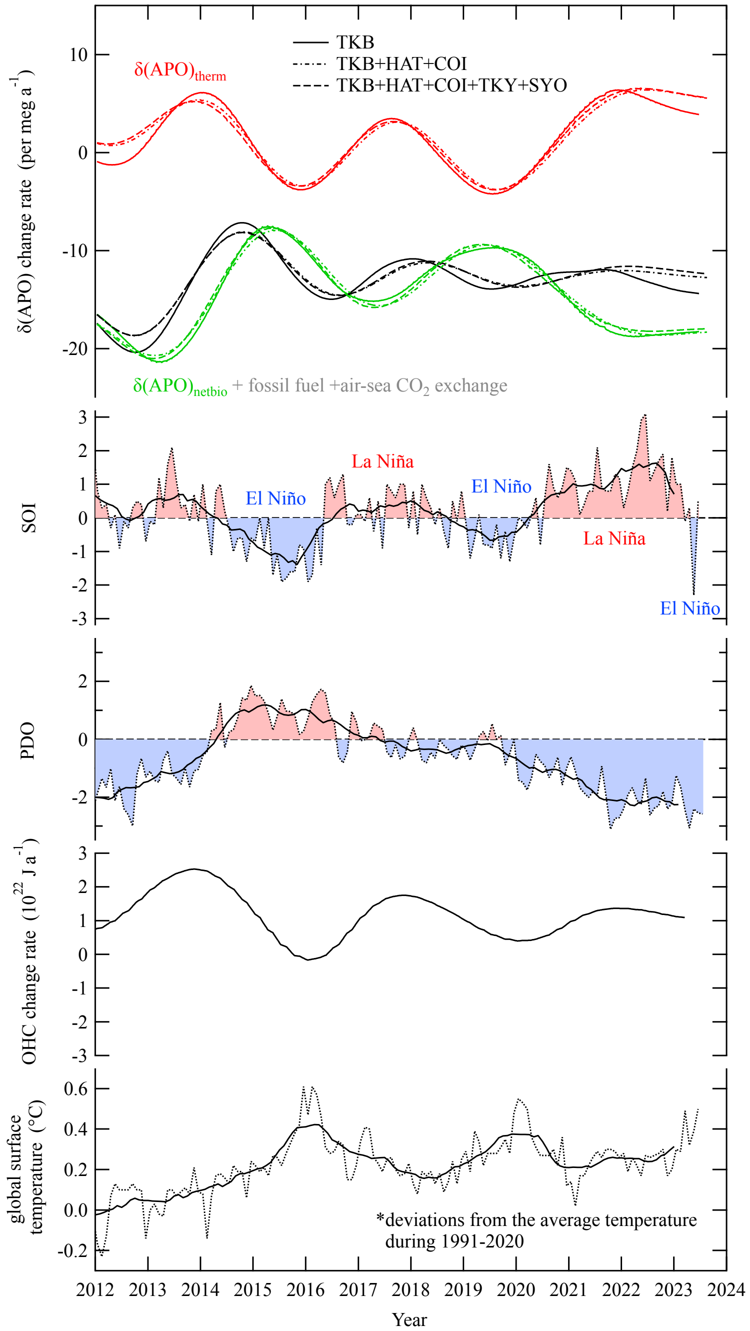

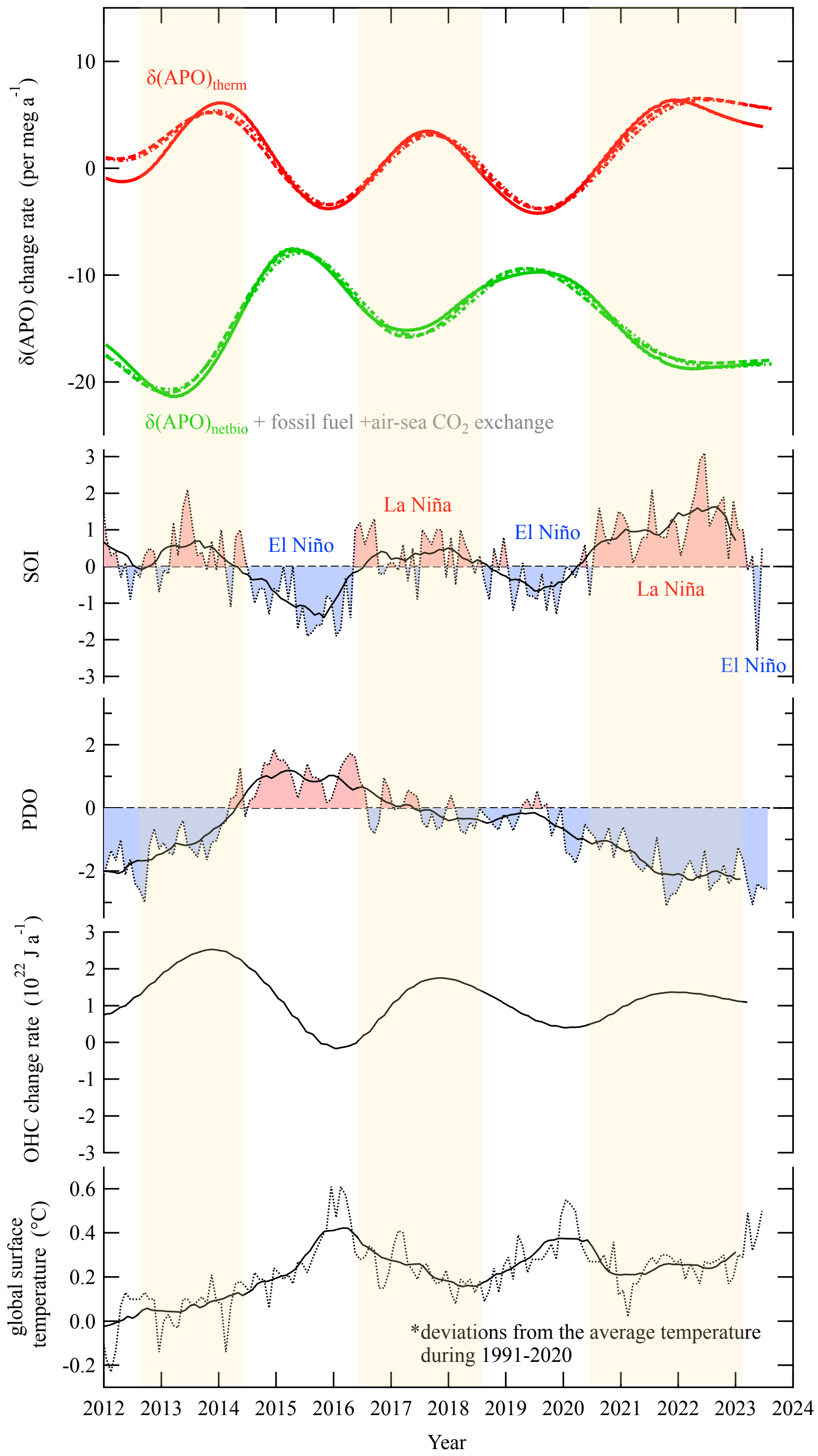

Annual change rate of δ(APO) due to the solubility change (δ(APO)$_{therm}$) from that due to the net marine biological activities (δ(APO)$_{netbio}$) by a combined analysis of δ(APO) and δ(Ar/N_2).

The annual change rate of the average δ(APO)$_{therm}$ was found to vary in phase with the Southern Oscillation Index (SOI) and the change rate of the global Ocean Heat Content (OHC).

On the other hand, the corresponding annual change rate of the average δ(APO)$_{netbio}$ varied in opposite phase with SOI. Similar features of δ(APO)$_{netbio}$ were found from our aircraft observations over MNM (Ishidoya et al., 2022).

These responses of δ(APO)$_{therm}$ and δ(APO)$_{netbio}$, to El Niño / La Niña events are qualitatively consistent with those expected from the simulations based on a community earth system model by Eddebbar et al. (2017).

The Earth tends to gain more energy during La Niña, mainly associated with reduction in outgoing longwave radiation (Loeb et al., 2012). Negative PDO also tends to strength La Niña condition. These characteristics seem to be consistent with the rapid increase of δ(APO)$_{therm}$ since the late 2020.

SOI and surface temperature data are from JMA website. https://www.data.jma.go.jp/cpd/data/elnino/index/dattab.html
https://www.data.jma.go.jp/cpdinfo/temp/mar_wld.html)
PDO and OHC data are from NOAA/NCEI website. https://www.ncei.noaa.gov/access/monitoring/pdo/
https://www.ncei.noaa.gov/access/global-ocean-heat-content/

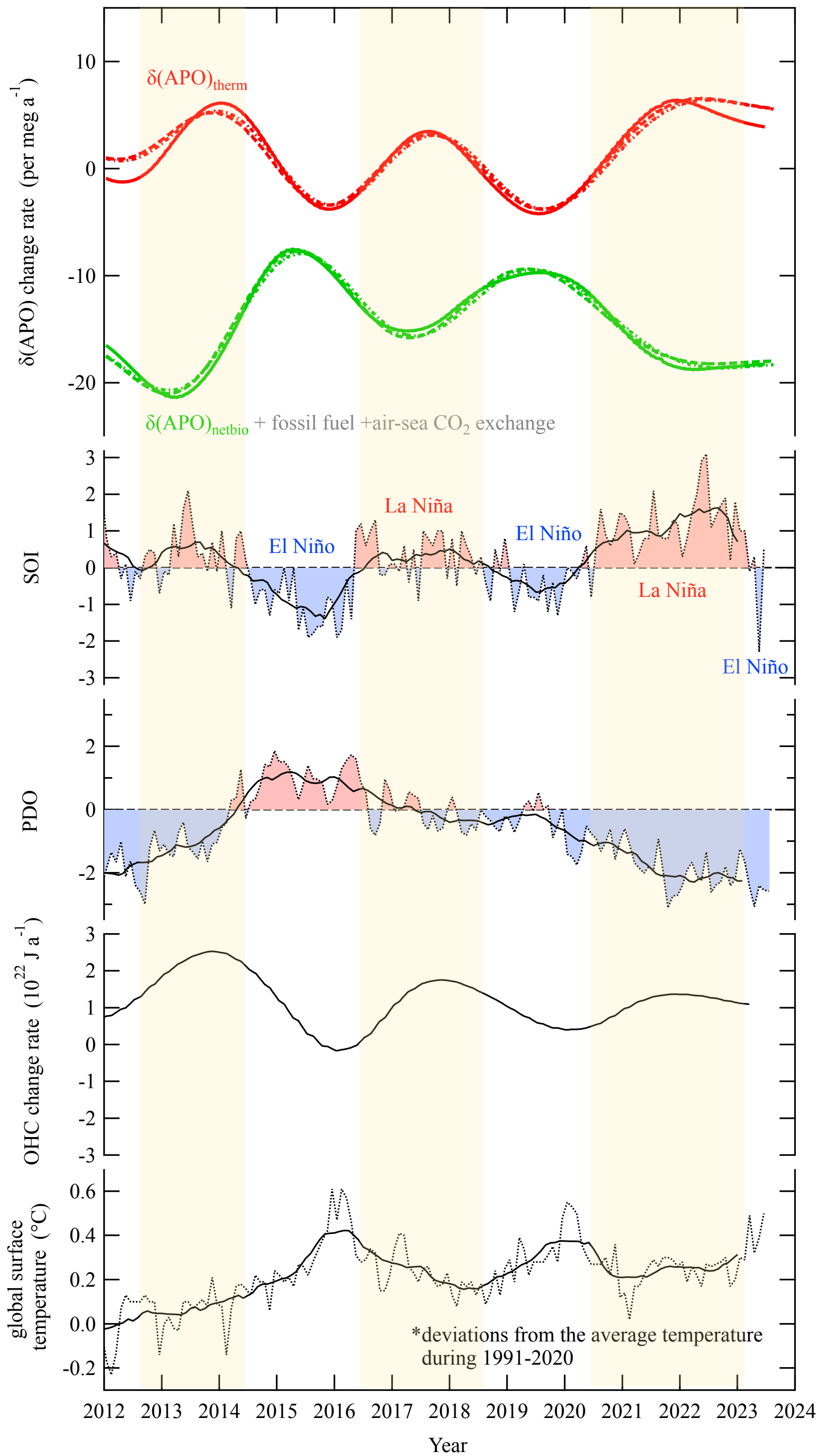
δ(APO)therm
δ(APO) change rate (per meg a-1)
δ(APO)netbio + fossil fuel +air-sea CO2 exchange
SOI
El Niño
La Niña
El Niño
La Niña
El Niño
PDO
OHC change rate (10^22 J a-1)
global surface temperature (°C)
*deviations from the average temperature during 1991-2020
2012 2013 2014 2015 2016 2017 2018 2019 2020 2021 2022 2023 2024
Year

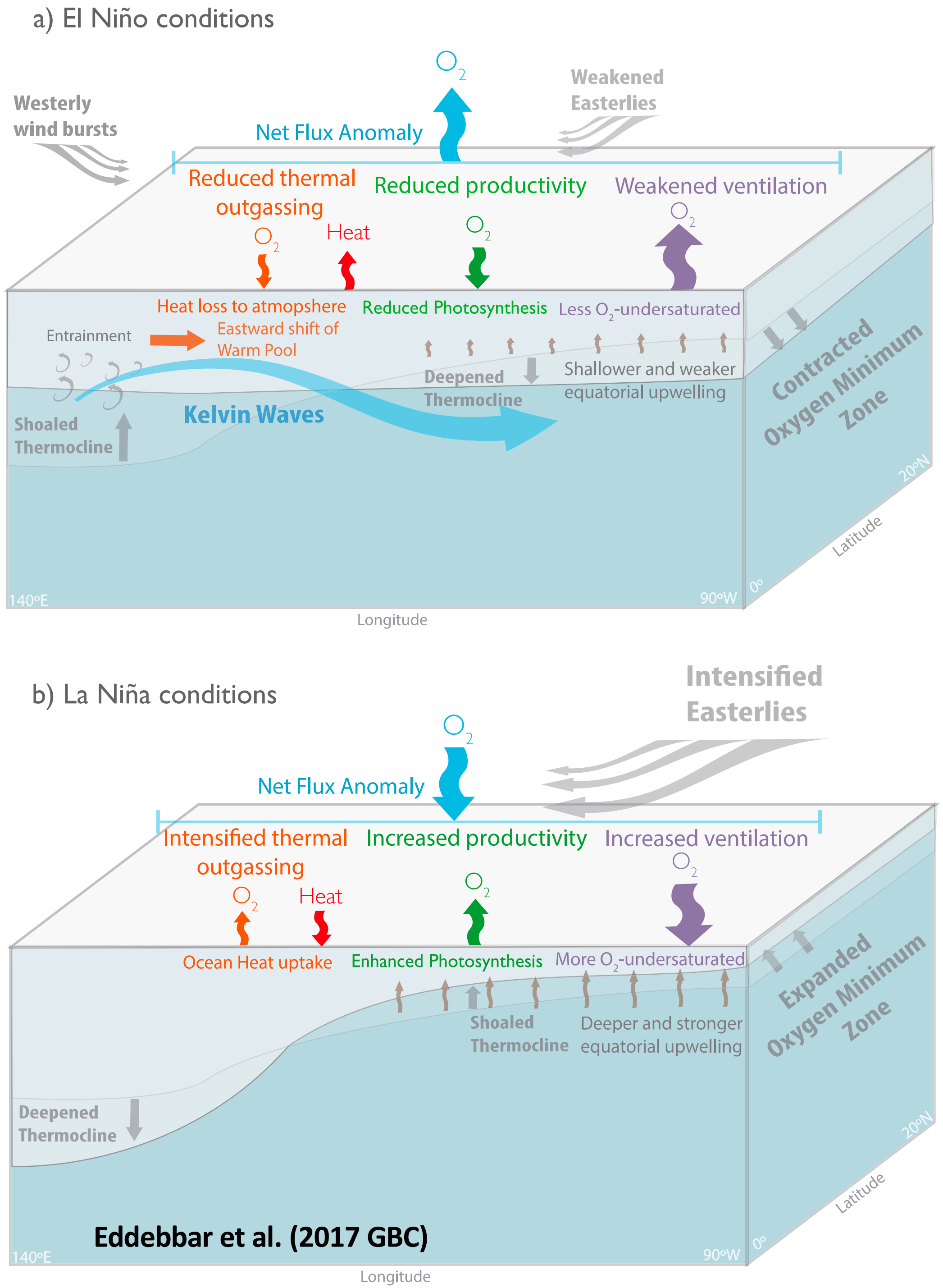
a) El Niño conditions
Westerly wind bursts
O2
Weakened Easterlies
Net Flux Anomaly
Reduced thermal outgassing
Reduced productivity
Weakened ventilation
Heat
Heat loss to atmopshere
Reduced Photosynthesis
Less O2-undersaturated
Entrainment
Eastward shift of Warm Pool
Deepened Thermocline
Shallower and weaker equatorial upwelling
Shoaled Thermocline
Kelvin Waves
Contracted Oxygen Minimum Zone
140°E
90°W
Longitude
Latitude
0°
20°N
b) La Niña conditions
Intensified Easterlies
Net Flux Anomaly
Intensified thermal outgassing
Increased productivity
Increased ventilation
Heat
Ocean Heat uptake
Enhanced Photosynthesis
More O2-undersaturated
Shoaled Thermocline
Deeper and stronger equatorial upwelling
Expanded Oxygen Minimum Zone
Deepened Thermocline
Eddebbar et al. (2017 GBC)
140°E
90°W
Longitude
Latitude
0°
20°N

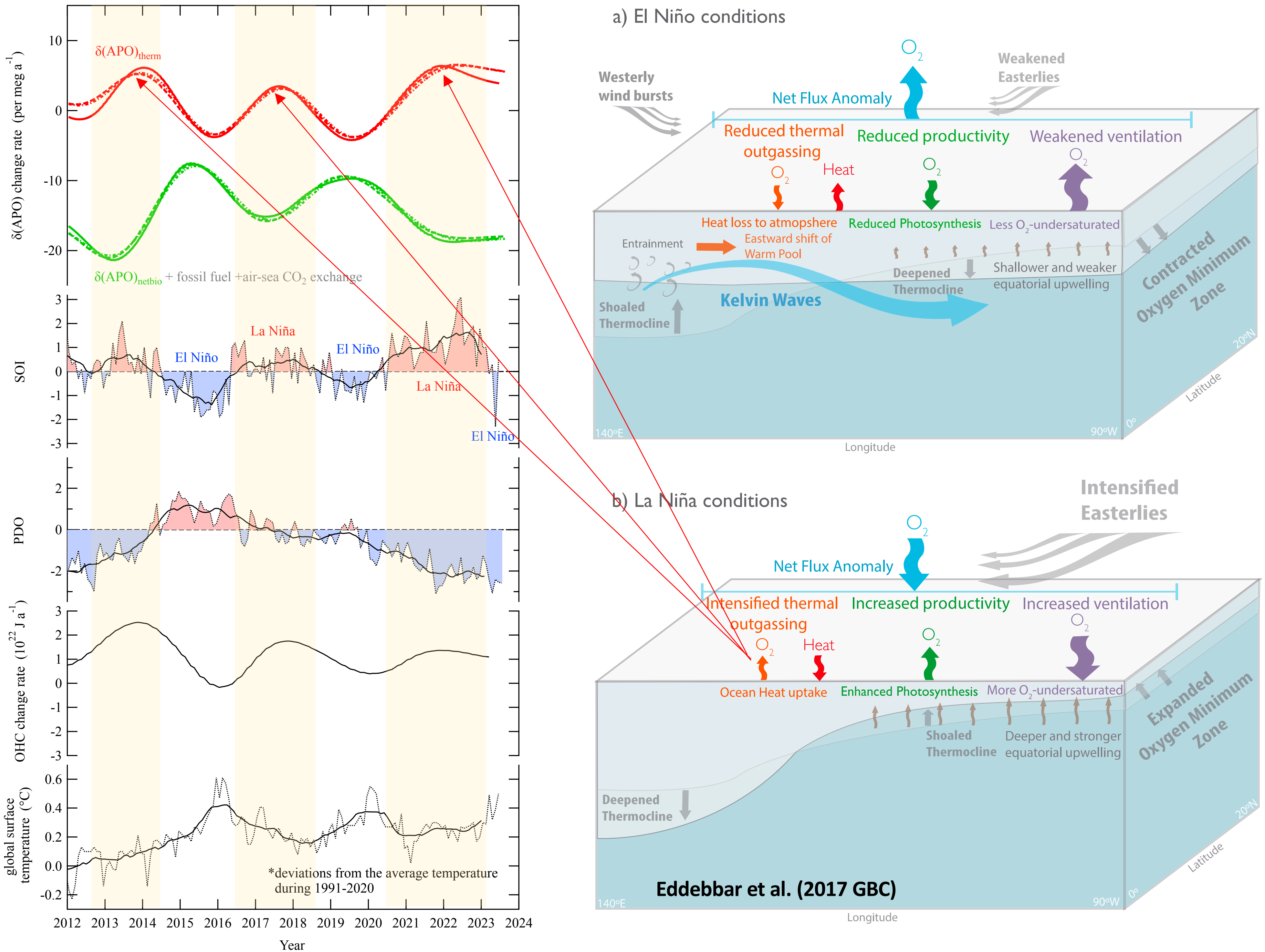

δ(APO)therm
δ(APO) change rate (per meg a⁻¹)
δ(APO)netbio + fossil fuel +air-sea CO2 exchange
SOI
La Niña
El Niño
El Niño
La Niña
El Niño
PDO
OHC change rate (10²² J a⁻¹)
global surface temperature (°C)
*deviations from the average temperature during 1991-2020
Year
a) El Niño conditions
O2
Weakened Easterlies
Westerly wind bursts
Net Flux Anomaly
Reduced thermal outgassing
Reduced productivity
Weakened ventilation
Heat
Heat loss to atmopshere
Reduced Photosynthesis
Less O2-undersaturated
Entrainment
Eastward shift of Warm Pool
Deepened Thermocline
Shallower and weaker equatorial upwelling
Kelvin Waves
Shoaled Thermocline
Contracted Oxygen Minimum Zone
140°E
90°W
Longitude
Latitude
20°N
0°
b) La Niña conditions
Intensified Easterlies
Net Flux Anomaly
Intensified thermal outgassing
Increased productivity
Increased ventilation
Heat
Ocean Heat uptake
Enhanced Photosynthesis
More O2-undersaturated
Shoaled Thermocline
Deeper and stronger equatorial upwelling
Expanded Oxygen Minimum Zone
Deepened Thermocline
Eddebbar et al. (2017 GBC)

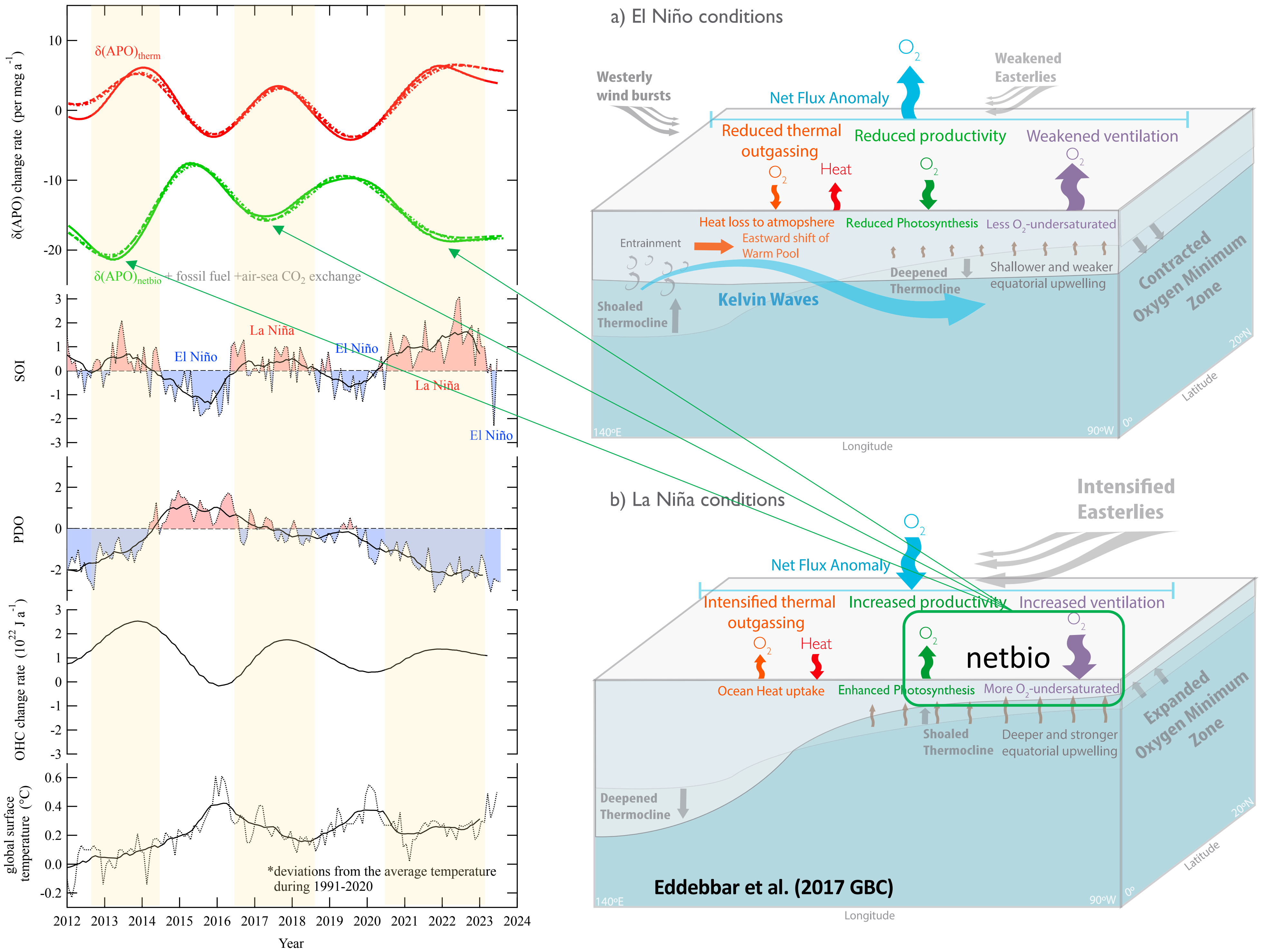

δ(APO)therm
δ(APO)netbio + fossil fuel +air-sea CO2 exchange
δ(APO) change rate (per meg a-1)
SOI
El Niño
La Niña
El Niño
La Niña
El Niño
PDO
OHC change rate (10^22 J a-1)
global surface temperature (°C)
*deviations from the average temperature during 1991-2020
Year
a) El Niño conditions
Westerly wind bursts
Net Flux Anomaly
Weakened Easterlies
Reduced thermal outgassing
Reduced productivity
Weakened ventilation
Heat
Heat loss to atmosphere
Reduced Photosynthesis
Less O2-undersaturated
Entrainment
Eastward shift of Warm Pool
Deepened Thermocline
Shallower and weaker equatorial upwelling
Kelvin Waves
Shoaled Thermocline
Contracted Oxygen Minimum Zone
Longitude
Latitude
b) La Niña conditions
Intensified Easterlies
Net Flux Anomaly
Intensified thermal outgassing
Increased productivity
Increased ventilation
netbio
Heat
Ocean Heat uptake
Enhanced Photosynthesis
More O2-undersaturated
Shoaled Thermocline
Deeper and stronger equatorial upwelling
Expanded Oxygen Minimum Zone
Deepened Thermocline
Eddebbar et al. (2017 GBC)
Longitude
Latitude

Outline

Brief introduction of our recent project

Variations in Ar/N_2 and APO at some surface stations since 2012

Gravitational separation in the stratosphere over Japan since 1988

Combined analysis of the surface and the stratospheric Ar/N_2 trends

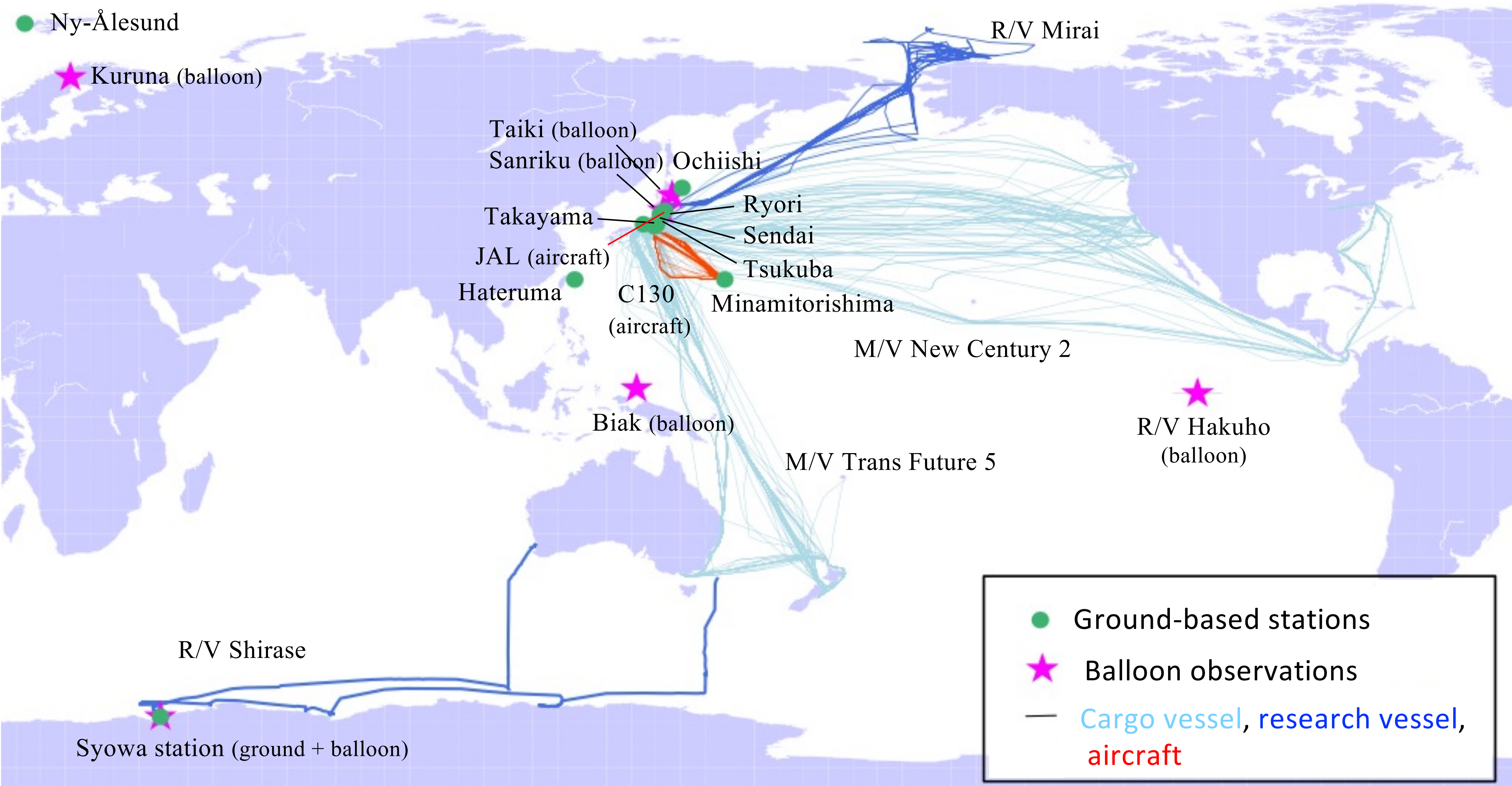
Ny-Ålesund
Kuruna (balloon)
R/V Mirai
Taiki (balloon)
Sanriku (balloon)
Ochiishi
Ryori
Takayama
Sendai
JAL (aircraft)
Tsukuba
Hateruma
C130
(aircraft)
Minamitorishima
M/V New Century 2
Biak (balloon)
R/V Hakuho
(balloon)
M/V Trans Future 5
R/V Shirase
Syowa station (ground + balloon)
Ground-based stations
Balloon observations
Cargo vessel, research vessel,
aircraft

The sites where balloon observations for gravitational separation in the stratosphere, evaluated based on $\delta(Ar/N_2)$, $\delta^{15}N$, $\delta^{18}O$ and $\delta^{40}Ar$, have been conducted

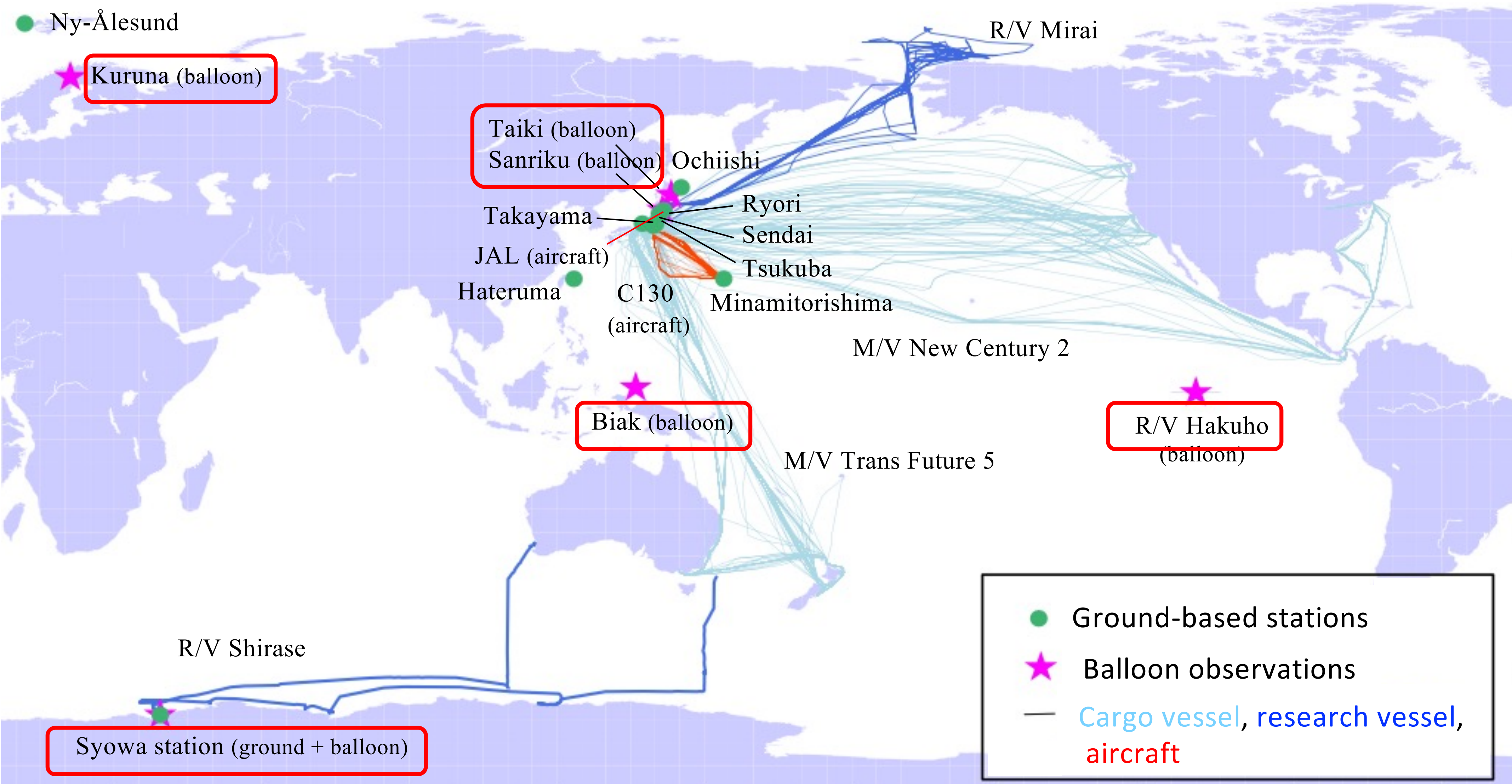

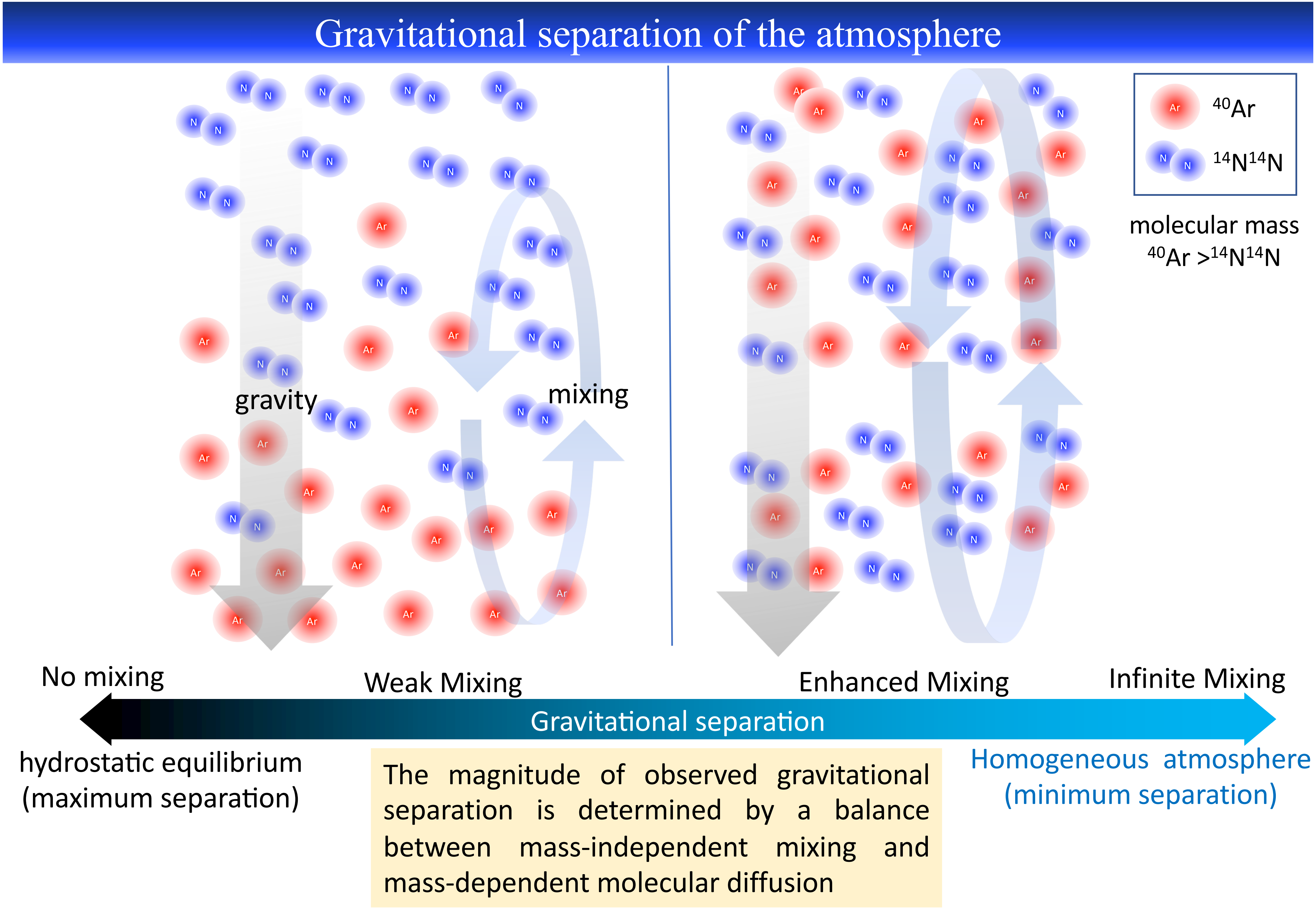

Gravitational separation of the atmosphere
gravity
mixing
Ar
N
^{40}Ar
^{14}N^{14}N
molecular mass
^{40}Ar >^{14}N^{14}N
No mixing
Weak Mixing
Enhanced Mixing
Infinite Mixing
Gravitational separation
hydrostatic equilibrium
(maximum separation)
Homogeneous atmosphere
(minimum separation)
The magnitude of observed gravitational separation is determined by a balance between mass-independent mixing and mass-dependent molecular diffusion

Balloon-borne cryogenic air sampler

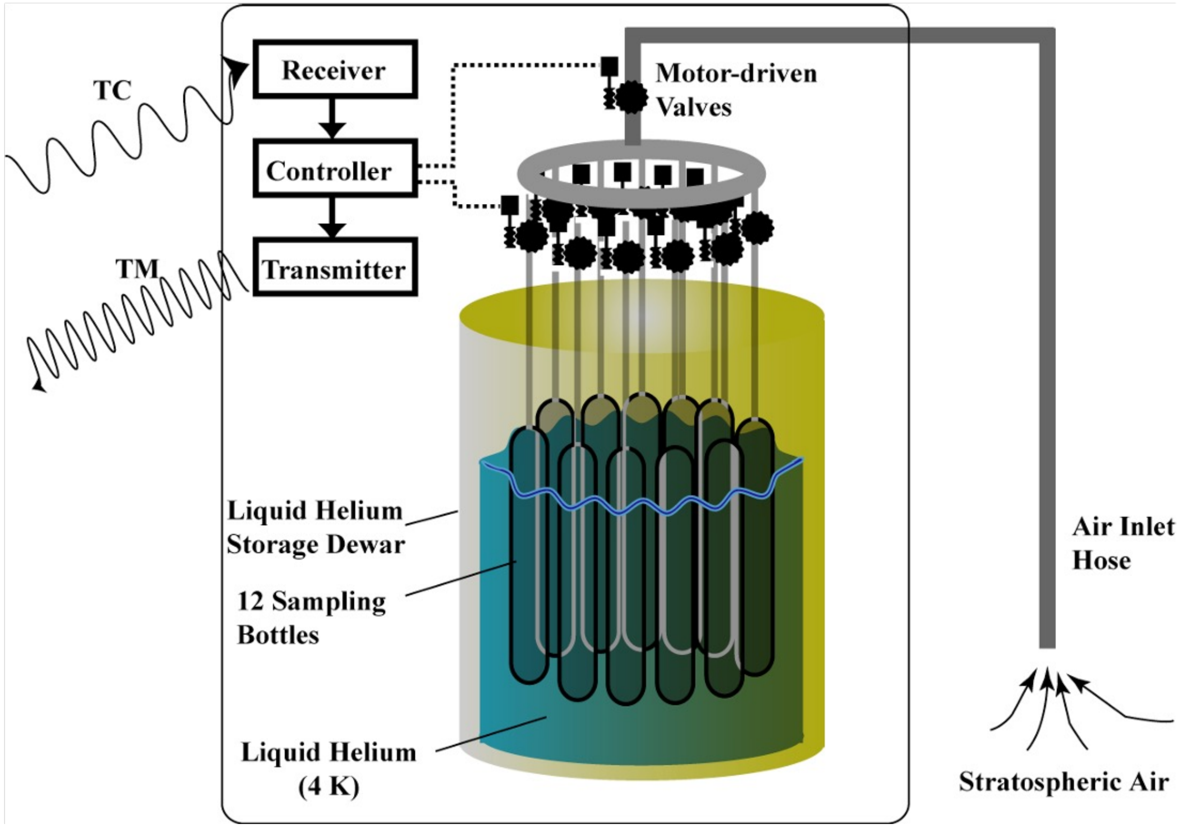

Balloon-borne whole air sampling

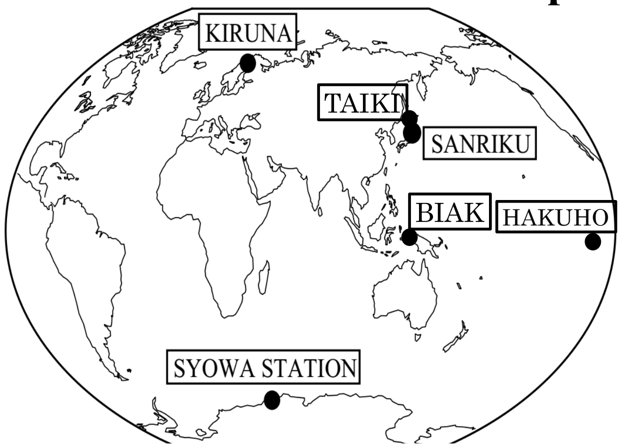

JAXA Balloon launch site
Sanriku: 1985～2007
Taiki: 2010～

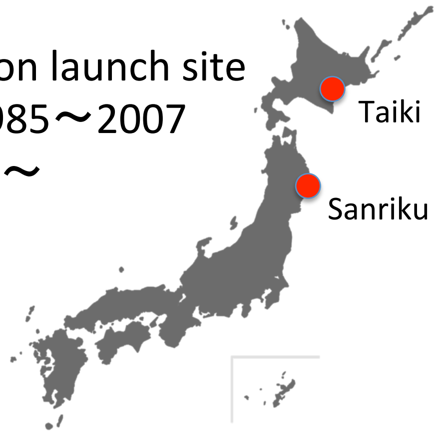

Nakazawa et al. (1995), Honda at el. (1996), Sugawara et al. (1997), Aoki et al. (2003), Toyoda at el. (2004) , Morimoto et al. (2009) etc.

Vertical profiles of gravitational separation and age of air observed over Japan, equatorial region, Arctica and Antarctica (updated from Ishidoya et al., 2008, 2013, 2018; Sugawara et al., 2018)

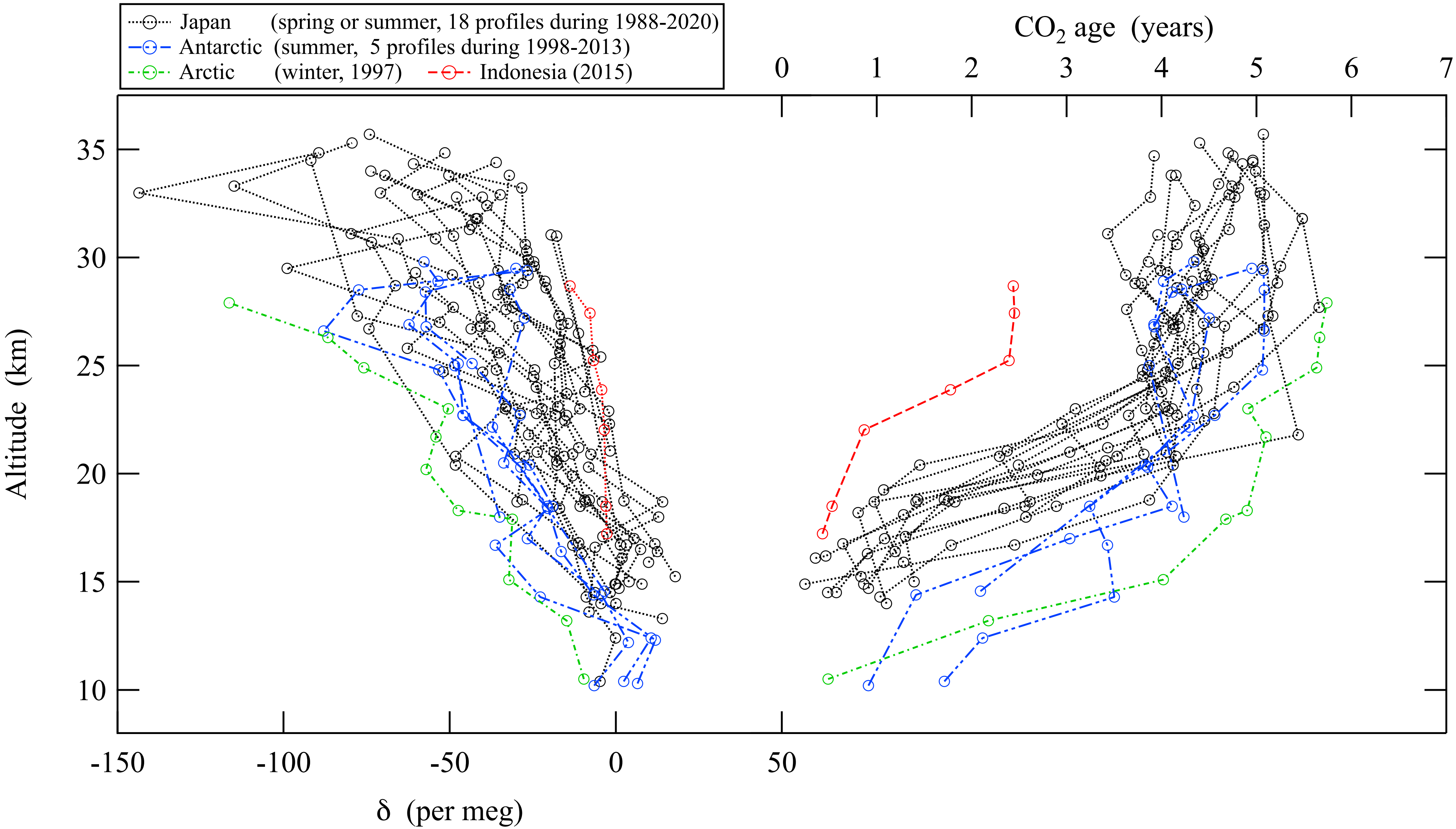

δ: Indicator of gravitational separation

$$\delta = \frac{1}{4}\left[\delta^{15}N + \delta^{18}O/2 + \delta^{40}Ar/4 + \delta\left(Ar/N_2\right)/12\right]$$

Vertical profiles of gravitational separation and age of air observed over Japan, equatorial region, Arctica and Antarctica (updated from Ishidoya et al., 2008, 2013, 2018; Sugawara et al., 2018)

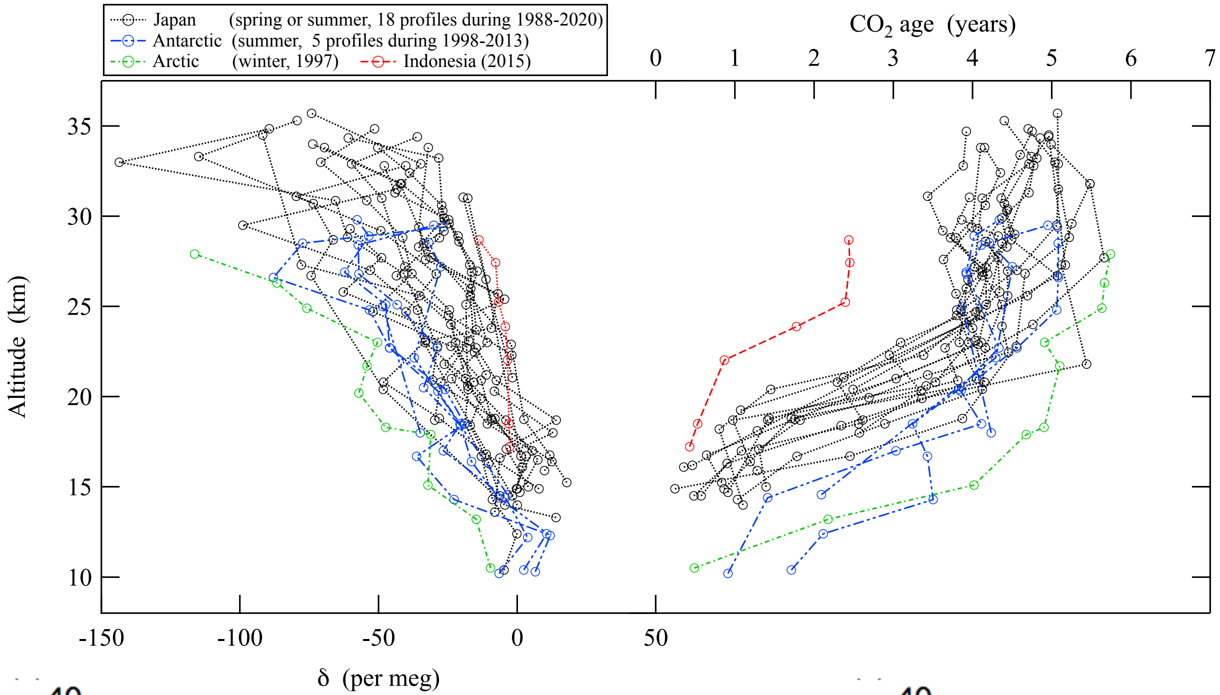

To interpret spatiotemporal variations in gravitational separation and mean age of air, we carried out 2-D and 3-D model simulation using SOCRATES and NIES-TM, respectively (e.g. Sugawara et al., 2018; Belikov et al., 2019). For this purpose, molecular-diffusion process from the surface to the middle atmosphere was incorporated.

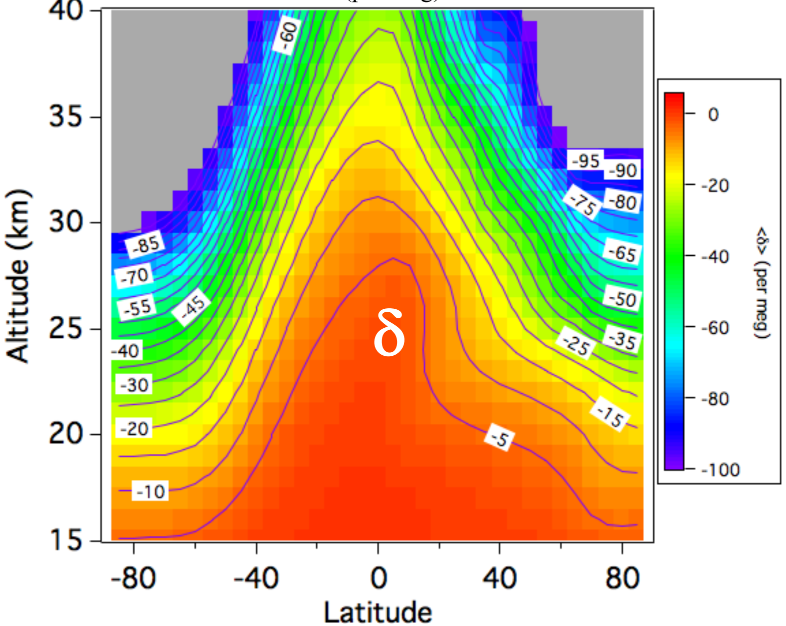

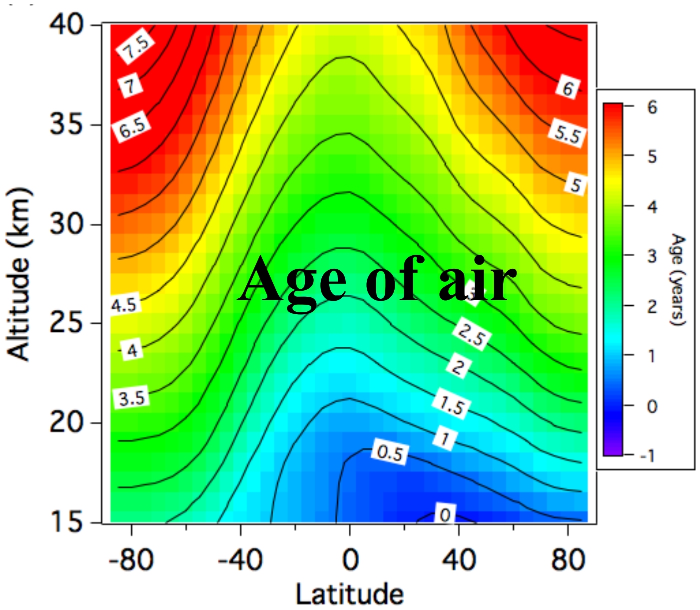

Both models reproduced general characteristics of the observed latitudinal variations seen in the vertical profiles over Japan, equatorial region, Arctic and Antarctica.

Long-term changes in gravitational separation and age of air observed in the middle stratosphere over Japan for the period 1988 – 2020

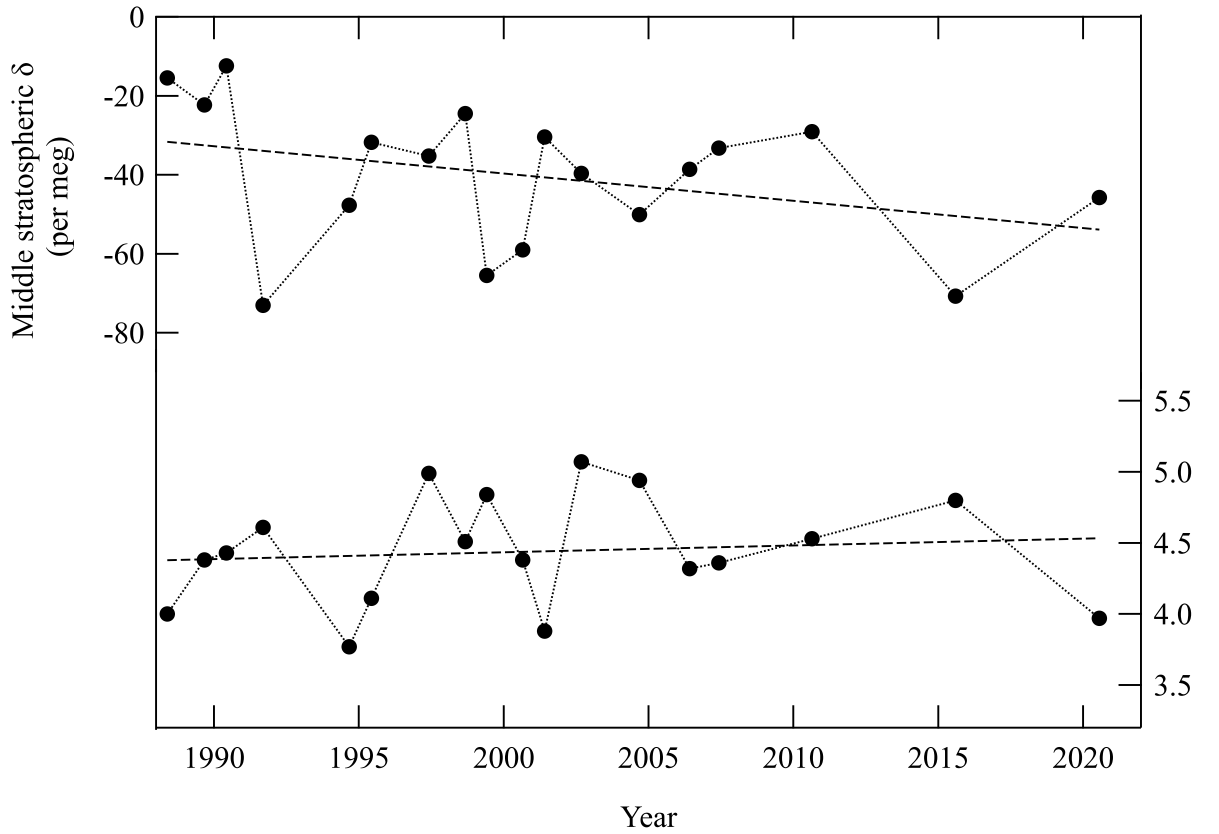

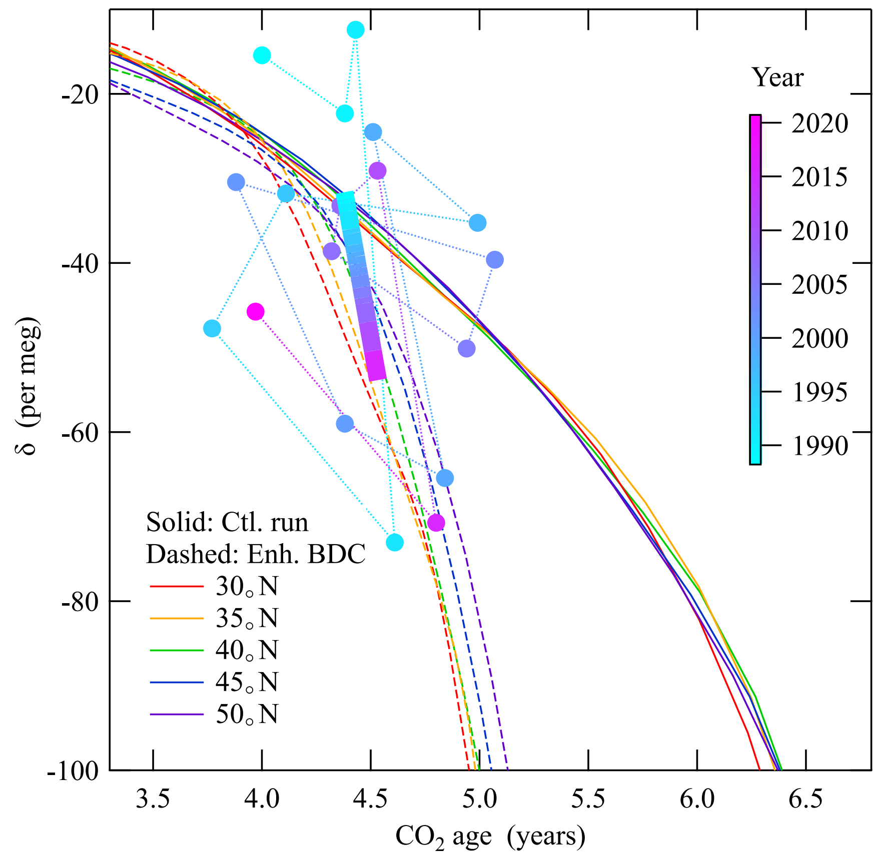

We found year-to-year changes in the δ were inversely correlated with that of the mean age. Based on similar analysis by Ishidoya et al. (2013), <u>secular enhancement of the Brewer-Dobson circulation (BDC) is suggested</u> from the relationships between the observed long-term changes in gravitational separation and those in mean age. It must be noted the “enhanced BDC run” by 2-D model (SOCRATES) simulation considered changes in mean stream function only. More realistic simulation by using 3-D model will be needed as a next step.

Outline

Brief introduction of our recent project

Variations in Ar/N_2 and APO at some surface stations since 2012

Gravitational separation in the stratosphere over Japan since 1988

Combined analysis of the surface and the stratospheric Ar/N_2 trends

Long-term trend in the surface δ(Ar/N_2) could also be modified by gravitational separation

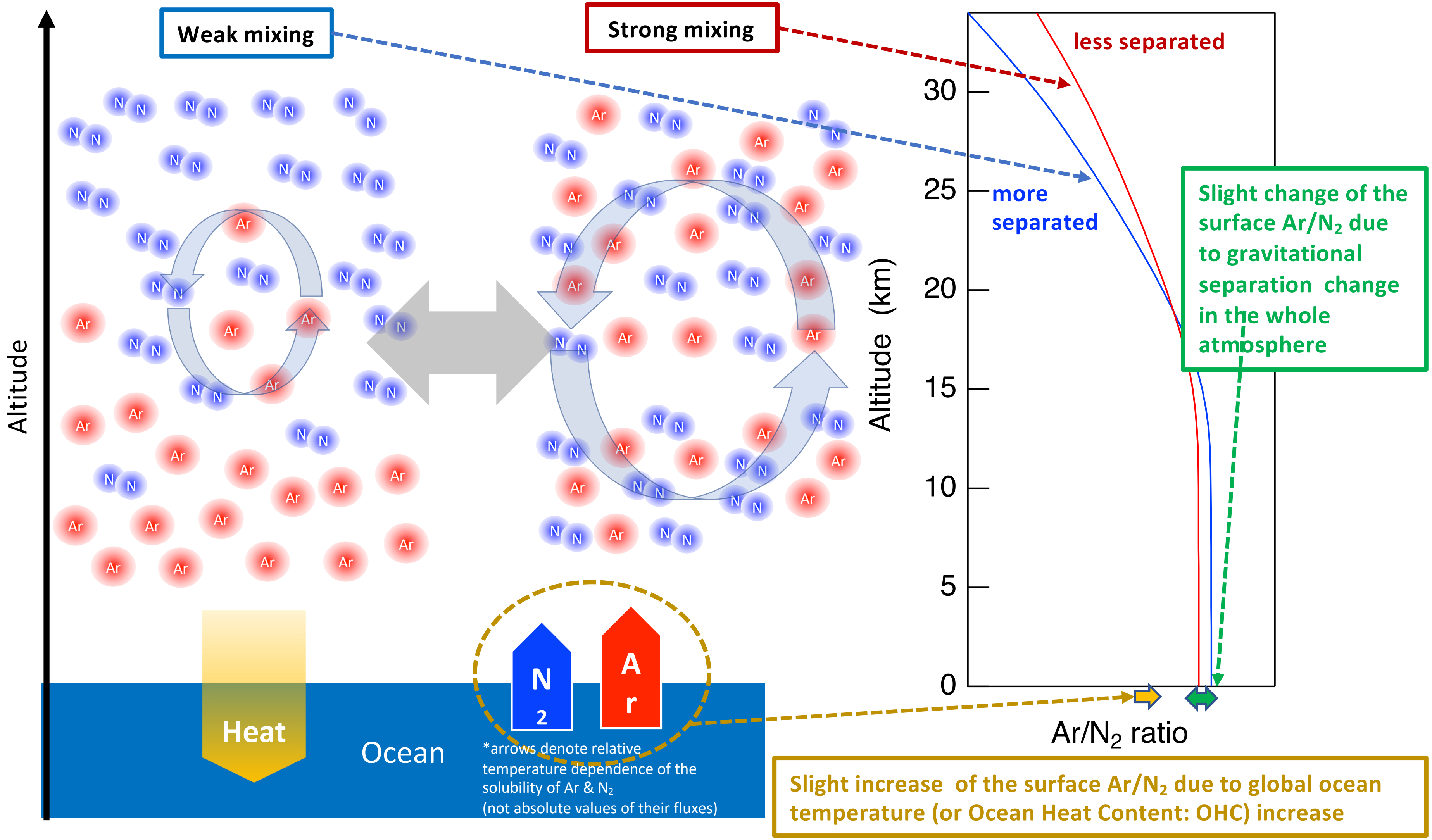

Gravitational separation is determined by a balance between molecular- and eddy-diffusion fluxes (e.g. Ishidoya et al., 2013; Sugawara et al., 2018). Therefore, if the atmospheric circulation is weakened, then the atmosphere is more separated and the surface δ(Ar/N_2) should increase slightly. If this effect is significant compared with the surface δ(Ar/N_2) increase by an ocean heat uptake, then simultaneous observations of the stratospheric and surface δ(Ar/N_2) must be important to evaluate ocean heat content (OHC) changes.

Ishidoya et al. (2021 ACP)

Secular enhancement of BDC, suggested from our observations and 2-D model simulations for gravitational separation and age of air, could cause slight secular decrease of the surface $\delta(Ar/N_2)$

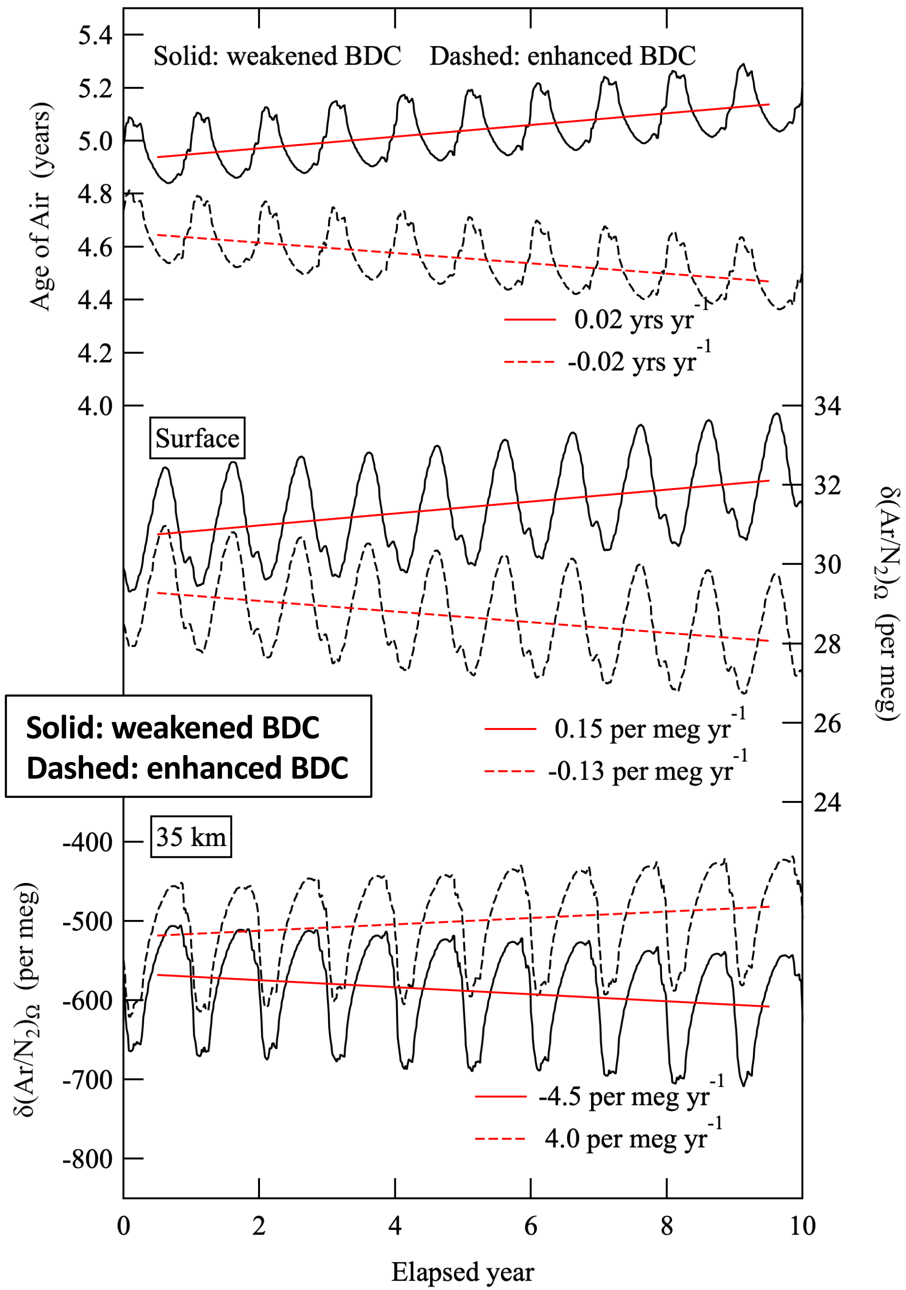

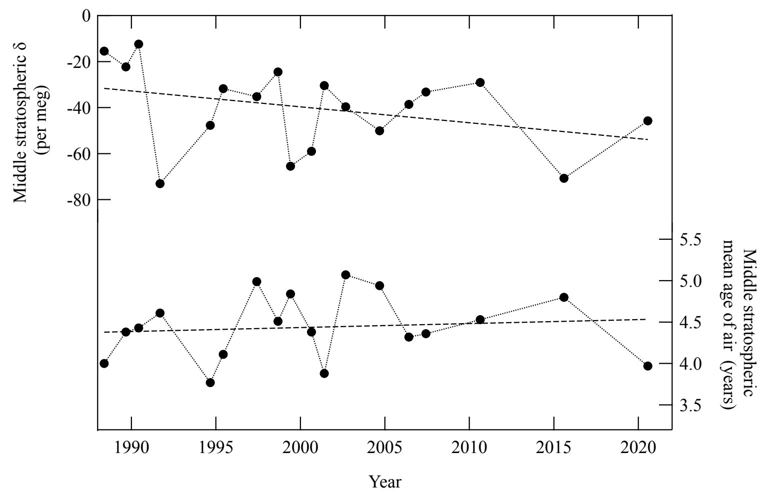

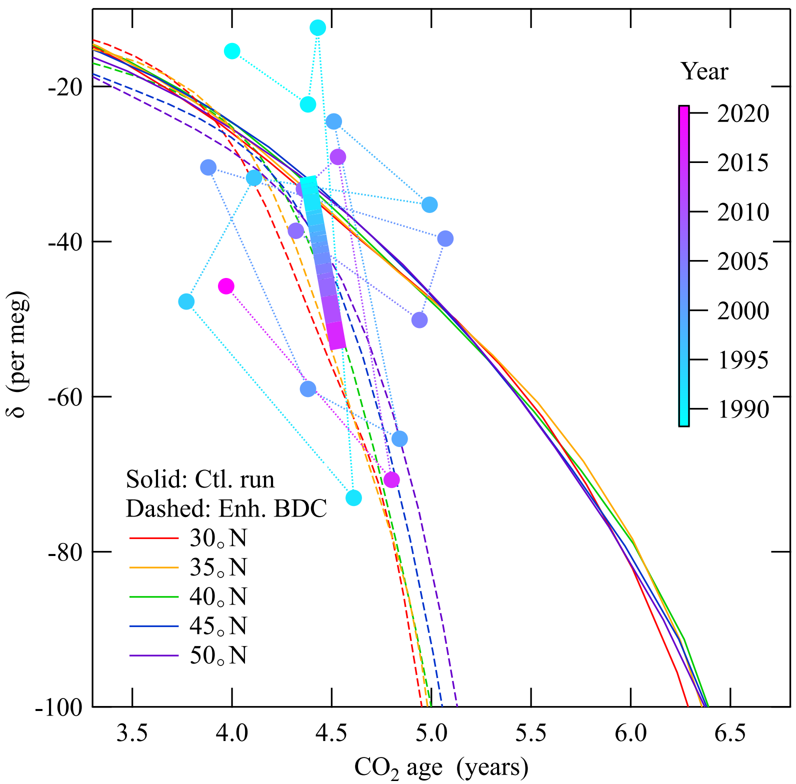

Secular enhancement of BDC, suggested from our observations and 2-D model simulations for gravitational separation and age of air, could cause slight secular decrease of the surface $\delta(Ar/N_2)$

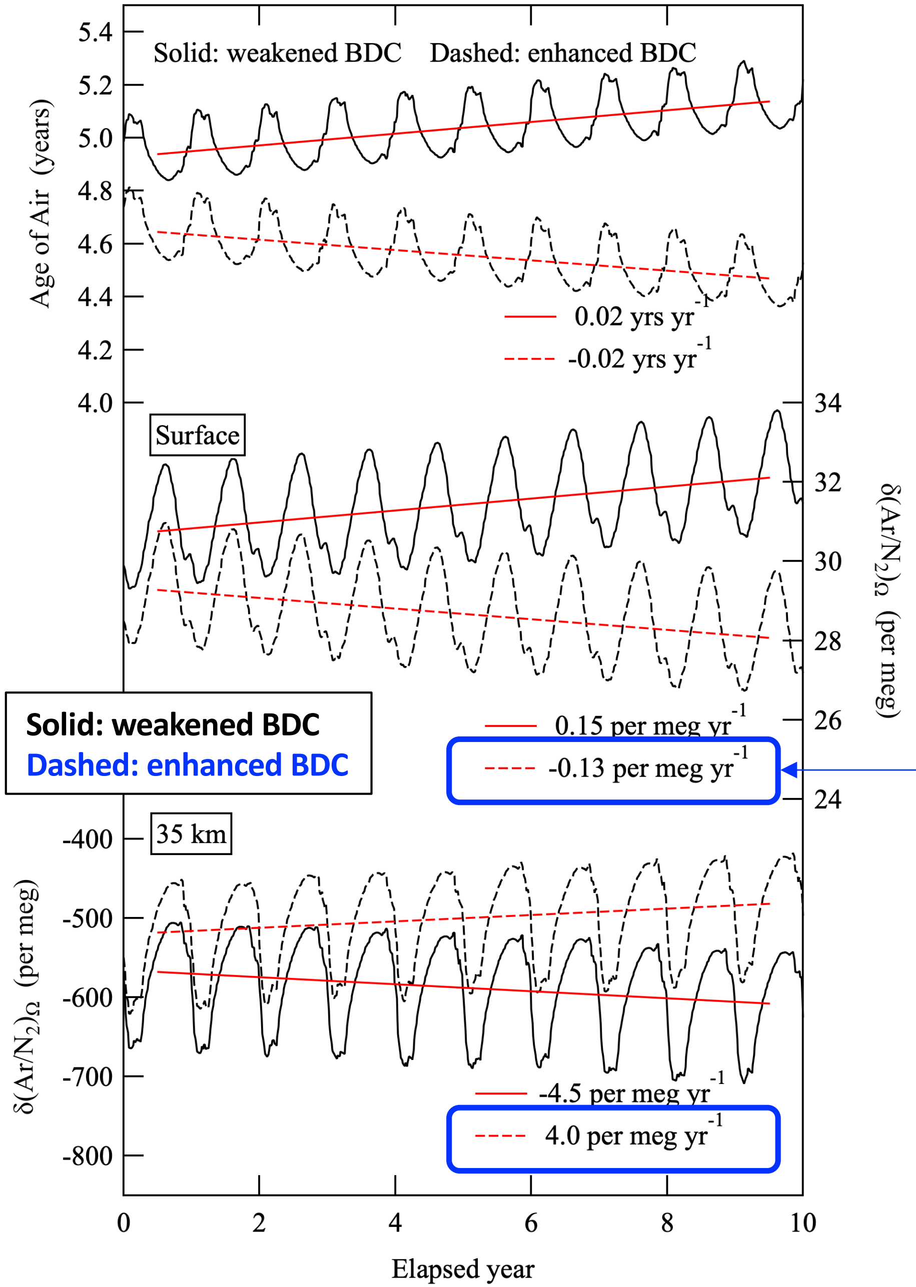

It is considered that gravitational separation throughout the atmosphere is weakened by secular enhancement of BDC. This results in secular increase and decrease of the stratospheric and the surface $\delta(Ar/N_2)$, respectively, based on our 2-D model simulation. However, it must be noted again the 2-D model simulation considered changes in mean stream function only, so that horizontal mixing processes are ignored. More realistic simulation by using 3-D model is needed.

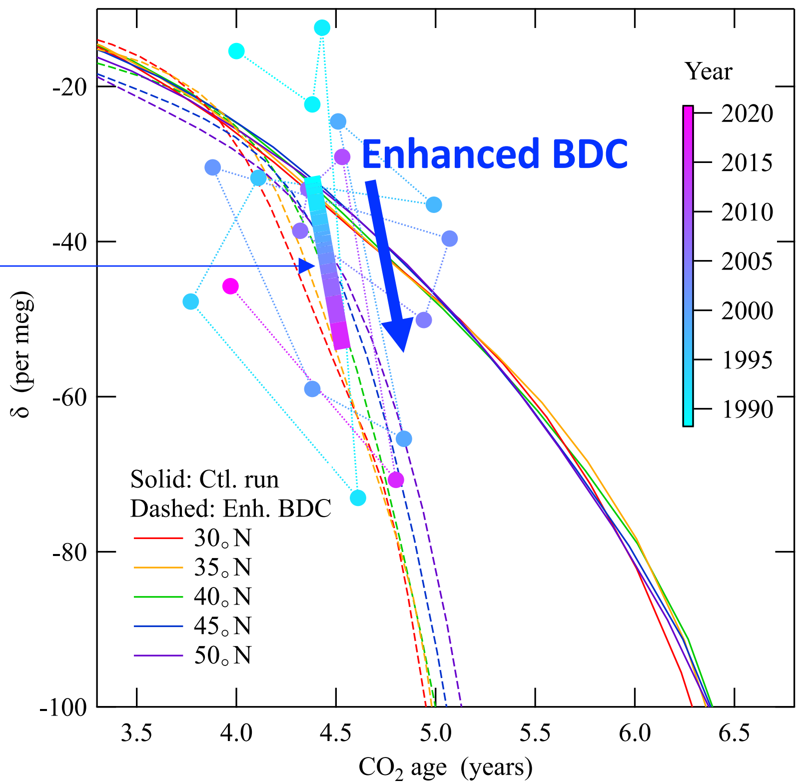

Secular trend in the surface δ(Ar/N_2) its application to the estimation of the global OHC increase

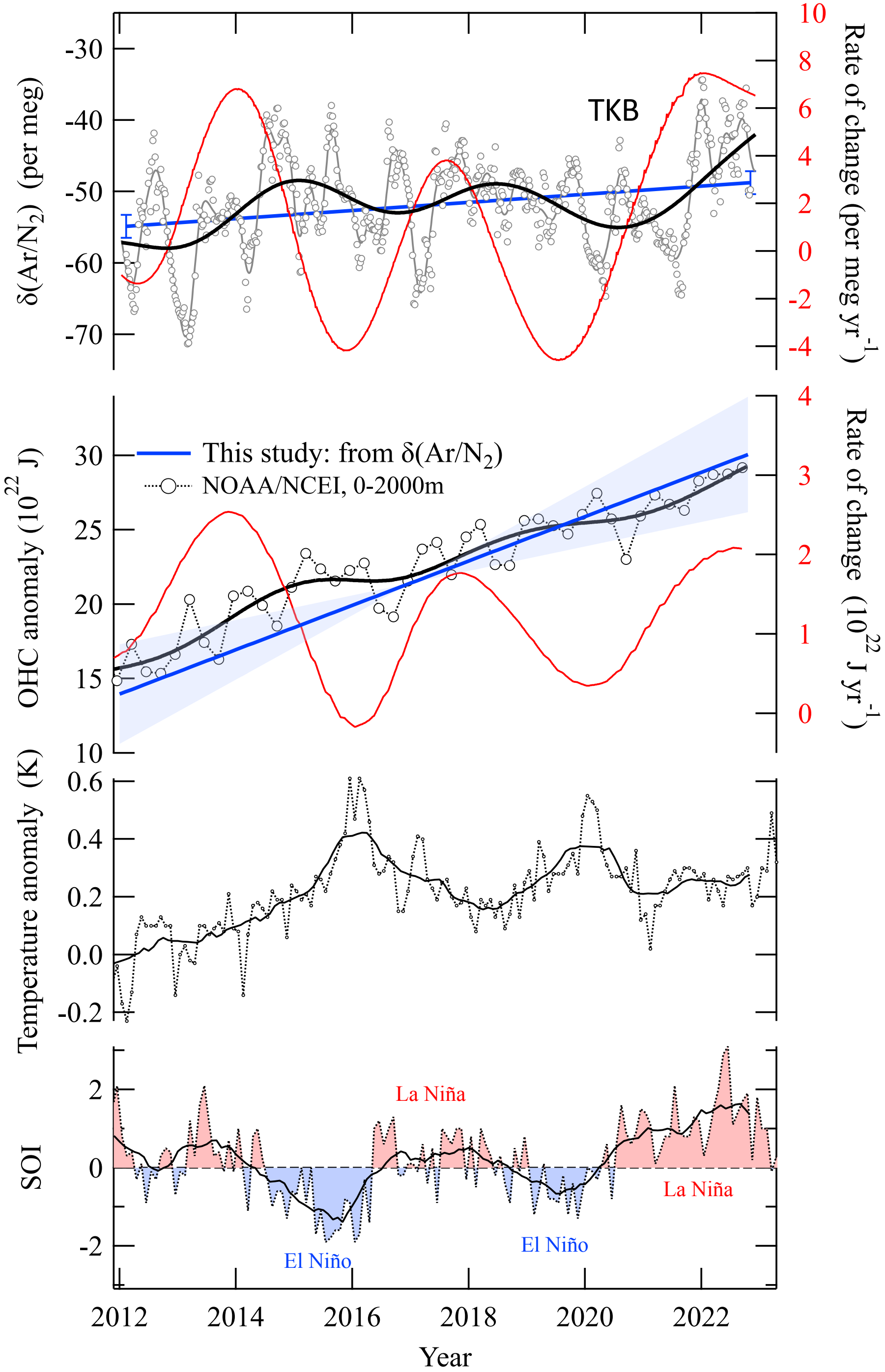

δ(Ar/N_2) at TKB, global OHC, global surface temperature, and SOI are shown in the figure. Rates of change of the δ(Ar/N_2) and OHC are also shown (red line). Both the rates show quite similar interannual variations. However, the ratio of "interannual variation / secular trend" for δ(Ar/N_2) is much larger than that for the OHC.

The linear secular trend of δ(Ar/N_2) is also shown in the figure (blue line). Considering the uncertainties around the regression and the long-term stability of the standard air, the trend is 0.5 ± 0.3 per meg/yr. The correction for gravitational separation changes expected from enhanced BDC, and that for technical issue associated with mass spectrometry we have re-evaluated recently are roughly in similar extent and in opposite direction, so that we adopt the trend of 0.5 per meg/yr as it is in this analysis.

The OHC increases based on δ(Ar/N_2) trend (blue line), assuming a conversion factor of 3.5×10^{-23} per meg per joule by assuming a one-box ocean with a temperature of 3.5° C, was roughly in consistent with that based on the ocean temperature measurements. The consistency suggests that the δ(Ar/N_2) is an important tracer for detecting spatiotemporally integrated changes in OHC and BDC.

Concluding remarks

Simultaneous observational results of δ(APO) and $\delta(Ar/N_2)$ at several sites since 2012 were presented. Variations in the annual change rates of $\delta(APO)_{therm}$ and $\delta(APO)_{netbio}$ were correlated with SOI and the change rates of the global OHC.

Long-term variations in gravitational separation in the lower-to-middle stratosphere for the period 1989-2020 were observed firstly. The vertical gradients of gravitational separation was found to vary roughly in opposite phase with the middle stratospheric mean age of air. If we follow the 2-D model simulation, then secular enhancement of the BDC is suggested.

The average OHC increase rates, estimated considering the secular trends in $\delta(Ar/N_2)$ and gravitational separation, was consistent with that reported by ocean temperature measurements. However, there are many issues left unsolved, and more studies are needed to understand detail mechanisms of the spatiotemporal variations in $\delta(Ar/N_2)$ and gravitational separation.

Acknowledgements

We thank the Scientific Ballooning (DAIKIKYU) Research and Operation Group of the Institute of Space and Astronautical Science, JAXA, staff of Global Environmental Forum (GEF), Japan Meteorological Agency (JMA), and Japanese Antarctic Research Expedition (JARE) for their works to collect the air samples at Hateruma and Ochiishi (GEF), Ryori and Minamitorishima (JMA), and Syowa station (JARE), respectively. This study was partly supported by the JSPS KAKENHI (grant nos. 23H00513, 22H05006, 19H01975 and 19K03963), Arctic Challenge for Sustainability II (ArCS-II), the Global Environment Research Coordination System from the Ministry of the Environment, Japan (grant nos. METI1454, METI1953, and MOE1951).